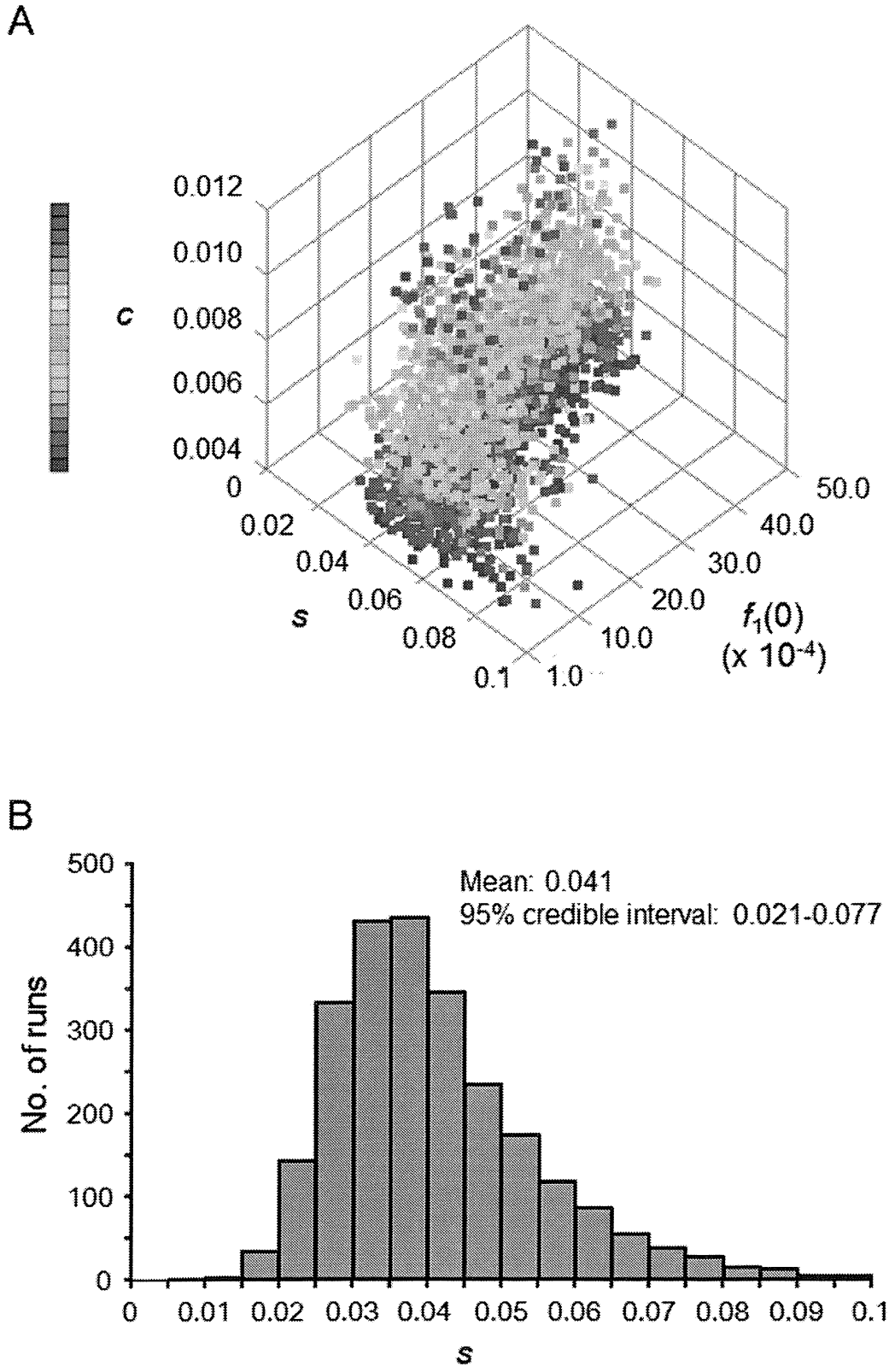

Figure 6. Estimation of model parameters for positive selection acting on *DPB1*04:01*. The recombination rate (*c*), initial haplotype frequency ($f_1(0)$), and selection coefficient (*s*), were estimated by comparing the four haplotype frequencies observed in our study population with the respective values predicted via simulation. (A) Posterior distributions of the three parameters that produced simulated data that resemble the observed data. (B) Frequency distribution of *s* accepted in simulation runs. The mean and 95% credible interval of *s* are 0.041 and 0.021−0.077.
doi:10.1371/journal.pone.0046806.g006

alleles that have been subject to geographically-restricted positive selection and to understand the role of *HLA* genes in the adaptation of human population to local environments over evolutionary time.

To estimate the selection coefficient of *DPB1*04:01*, we used a simple two-locus two-allele genetic model that was based on two assumptions, directional selection at *DPB1* and selective neutrality at *HLA-DQB1*. The problem associated with the use of this model was that the Ewens-Watterson test revealed that the allele frequency distribution at *HLA-DQB1* in this study population deviated significantly from that expected under neutrality (Table 2); therefore, the assumption of selective neutrality at *HLA-DQB1* may not be valid. If balancing selection is operating at *HLA-DQB1*, the allele frequency of *DQB1*06:04* is maintained at a certain frequency, and the change in the allele frequency of *DPB1*04:01* must be influenced by this selection at *HLA-DQB1*, although the effect of balancing selection at *HLA-DQB1* on the estimation of s is considered to be much smaller than that of directional selection favoring *DPB1*04:01*.

In this study, six *HLA* loci were investigated in 418 Japanese subjects. Of *HLA* alleles with high population frequencies, *DPB1*04:01*, which was present in the most common 6-locus *HLA* haplotype spanning more than 4 Mb, showed exceptionally high *HH*. A computer simulation estimated the selection coefficient of *DPB1*04:01* as 0.041. Taken together with high *HH* value of *DPB1*04:01*, we conclude that *DPB1*04:01* has recently undergone strong positive selection in Japanese population.

Materials and Methods

Subjects

All 418 individuals investigated in this study were unrelated Japanese adults living in Tokyo or neighboring areas. The genomic DNAs were extracted from peripheral blood samples using a commercial kit (QIAamp Blood Kit [Qiagen, Hilden, Germany]). All blood and DNA samples were de-identified. Verbal informed consent was obtained from all the participants before 1990. In this study, written informed consent was not obtained because the blood sampling was conducted before the "Ethical Guidelines for Human Genome and Genetic Sequencing Research" were established in Japan. Under the condition that DNA sample is permanently de-linked from the individual, this study was approved by the Research Ethics Committee of the Faculty of Medicine, University of Tokyo.

HLA Typing

DNA typing of *HLA* alleles was performed by HLA LABORATORY (Kyoto, Japan) using a Luminex Multi-Analyte profiling system (xMAP; Luminex, Austin, TX, USA) [37].

SNP Typing

Five Japanese subjects who had at least one *A*33:03-C*14:03-B*44:03-DRB1*13:02-DQB1*06:04-DPB1*04:01* haplotype were genotyped using the Axiom™ Genome-Wide ASI 1 Array Plate (Affymetrix Inc., Santa Clara, CA, USA). Of five subjects, three subjects were homozygous for the *A*33:03-C*14:03-B*44:03-DRB1*13:02-DQB1*06:04-DPB1*04:01* haplotype and two subjects had the heterozygous genotypes of the *A*33:03-C*14:03-B*44:03-DRB1*13:02-DQB1*06:04-DPB1*04:01* haplotype and the *A*24:02-C*07:02-B*07:02-DRB1*01:01-DQB1*05:01-DPB1*04:02* haplotype and of the *A*33:03-C*14:03-B*44:03-DRB1*13:02-DQB1*06:04-DPB1*04:01* haplotype and the *A*24:02-C*12:02-B*52:01-DRB1*15:02-DQB1*06:01-DPB1*09:01* haplotype.

Statistical Analysis

Deviation from HWE for each *HLA* locus was tested using an exact test available in a web-based software, Genepop 4.0.10 [38]. Using Arlequin version 3.5 [39], the Ewens-Watterson test [40], which is based on Ewens sampling theory of neutral alleles [19], was performed to assess whether the observed distribution of allele frequencies at each *HLA* locus was different from an expectation that was based on neutrality.

To evaluate the degree of LD between *HLA* alleles, values of r^2 and D' [21] for all pairwise combinations of *HLA* alleles were calculated based on the haplotype frequencies estimated using the expectation maximization algorithm [20]. Here, each *HLA* allele was regarded as a single nucleotide polymorphism (SNP). For example, the *A*01:01* allele and the other alleles at the *HLA-A* locus were designated as "A" and "G", respectively. Accordingly, the algorithm for the estimation of haplotype frequencies for two loci, each with two alleles, could be applied to the *HLA* loci with multiple alleles for the purposes of these pairwise comparisons.

The LD parameter, 2-locus $|D'|$, between any two *HLA* loci (locus 1 and locus 2) was calculated based on the pairwise LD parameter, D'_{ij}, between ith allele at locus 1 and jth allele at locus 2 as follows: 2-locus $|D'| = \sum_{i=1}^{m} \sum_{j=1}^{n} p_i q_j |D'_{ij}|$, where p_i and q_j represent the frequencies of ith allele at locus 1 with m different alleles and jth allele at locus 2 with n different alleles. Spearman's rank correlation coefficient between 2-locus $|D'|$ and the physical distance was calculated. Assuming a model: 2-locus $|D'| = \left(1 - 0.67 \times 10^{-5} \times x\right)^a$, the curve fitting model parameter, a, was estimated using the least squares method; this method minimizes the sum-of-squared residual between an observed value and a fitted value that was determine by a model. In the above equation, the physical distance (Kb) between two loci is denoted by x and the recombination intensity in the *HLA* region was set at 0.65 cM/Mb [27,41].

The phased haplotypes consisting of two or more *HLA* loci were estimated using the PHASE program version 2.1 [25,26]. The estimated 6-locus haplotypes were further used for the calculation of extended haplotype homozygosity (*EHH*) [17] and of haplotype homozygosity (*HH*). In this study, *HH* of each *HLA* allele was defined as the probability that any two randomly chosen samples of haplotype bearing the *HLA* allele have the same 6-locus *HLA* haplotype.

A sliding window analysis of individual heterozygosity, which was defined as the proportion of heterozygous SNPs to SNPs genotyped in a single subject, was conducted to examine whether the *A*33:03-C*14:03-B*44:03-DRB1*13:02-DQB1*06:04-DPB1*04:01* haplotype had a single origin in Japan. 19,949 SNPs located on 6p were genotyped, and the average SNP density was 0.34 SNP/kb. The window and step sizes were 1 Mb and 200 kb, respectively. This analysis was performed using the SNP data from the five subject included in the SNP typing: three subjects were homozygous for the *A*33:03-C*14:03-B*44:03-DRB1*13:02-DQB1*06:04-DPB1*04:01* haplotype and two subjects had the heterozygous genotypes of the *A*33:03-C*14:03-B*44:03-DRB1*13:02-DQB1*06:04-DPB1*04:01* haplotype and the *A*24:02-C*07:02-B*07:02-DRB1*01:01-DQB1*05:01-DPB1*04:02* haplotype and of the *A*33:03-C*14:03-B*44:03-DRB1*13:02-DQB1*06:04-DPB1*04:01* haplotype and the *A*24:02-C*12:02-B*52:01-DRB1*15:02-DQB1*06:01-DPB1*09:01* haplotype.

Computer Simulation

To estimate the intensity of recent positive selection acting on *DPB1*04:01*, a stochastic population genetic model (two-locus two-allele model) assuming both positive selection and random

genetic drift was built and assessed. The diploid population size, N, was set to be 10,000 (i.e., 20,000 chromosomes). Four haplotypes carrying *DPB1*04:01* or non-*DPB1*04:01* alleles (designated by *DPB1*X*) at the *HLA-DPB1* locus and *DQB1*06:04* or non-*DQB1:06:04* alleles (designated by *DQB1*X*) at the *HLA-DQB1* locus were used in this model. The frequencies of the *DQB1*06:04-DPB1*04:01*, *DQB1*X-DPB1*04:01*, *DQB1*06:04-DPB1*X*, and *DQB1*X-DPB1*X* haplotypes at generation t were denoted by $f_1(t)$, $f_2(t)$, $f_3(t)$, and $f_4(t)$, respectively. The current frequencies of the corresponding haplotypes in our study population were denoted by f_1, f_2, f_3, and f_4. A dominant selection was assumed for *DPB1*04:01* (i.e., relative finesses of *DPB1*04:01/DPB1*04:01*, *DPB1*04:01/DPB1*X*, and *DPB1*X/DPB1*X* are 1, 1, and 1 - s, respectively). The initial haplotype frequencies were set as $f_1(t) = z, f_2(t) = 0, f_3(t) = (1-z)f_3/(f_3+f_4)$, and $f_4(t) = (1-z)f_4/(f_3+f_4)$. The recombination between *HLA-DPB1* and *HLA-DQB1* loci was assumed to occur at a rate of c. Since the recombination rate between *HLA-DQB1* and *HLA-DPB1* has been estimated to be between 0.004 and 0.012 [41,42], a uniform recombination rate (c) within this range was used as a prior distribution. To estimate suitable parameter sets of z, s, and c, each value was drawn by a random number generator in every simulation run. The random numbers were between 0.0001 (i.e., $2/2N$) and 0.005 (i.e., $100/2N$) for z, between 0 and 0.1 for s, and between 0.004 and 0.012 for c.

Next, to evaluate the similarity between simulated and observed frequencies,

$$e = \sum_{i=1}^{4} \frac{(f_i(t) - f_i)^2}{f_i(t) + f_i}$$

was calculated. As the simulated haplotype frequencies, $f_1(t)$, $f_2(t)$, $f_3(t)$, and $f_4(t)$, approaches values close to the observed frequencies, f_1, f_2, f_3, and f_4, the value of e approaches 0. The rejection method [18,32,33] was used to accept only simulation runs that resulted in (i) e of less than 0.01, (ii) $f_1(t)$ of not less than $f_1 - 0.01$ nor more than $f_1 + 0.01$, and (iii) t of not less than 92 nor more than 115 generations. A total of 2,500 runs were accepted. The mean and 95% credible interval of s were obtained from the 2,500 accepted runs.

Supporting Information

Data S1 Pairwise LD measures for individual HLA allele pairs.
(XLSX)

Table S1 Linkage Disequilibrium between pairs of HLA loci.
(XLSX)

Table S2 Estimated frequencies of 2-locus HLA haplotypes.
(XLSX)

Table S3 Estimated frequencies of 3-locus HLA haplotypes.
(XLSX)

Table S4 Estimated frequencies of 4-locus HLA haplotypes.
(XLSX)

Table S5 Estimated frequencies of 5-locus HLA haplotypes.
(XLSX)

Acknowledgments

We deeply thank all the subjects for their participation in the study. We also thank Ms Yoriko Mawatari, Ms Megumi Sageshima, Ms Yuko Ogasawara, Ms Natsumi Baba, and Ms Rieko Hayashi (University of Tokyo) for technical assistance.

Author Contributions

Conceived and designed the experiments: MK JO. Performed the experiments: MK NN. Analyzed the data: MK JO. Contributed reagents/materials/analysis tools: JO NN KT. Wrote the paper: MK JO. Assembled the data: MK NN. Performed the computer simulation: JO.

References

1. Bjorkman PJ, Saper MA, Samraoui B, Bennett WS, Strominger JL, et al. (1987) The foreign antigen binding site and T cell recognition regions of class I histocompatibility antigens. Nature 329: 512–518.
2. Campbell RD, Trowsdale J (1993) Map of the human MHC. Immunology today 14: 349–352.
3. Takahata N, Nei M (1990) Allelic genealogy under overdominant and frequency-dependent selection and polymorphism of major histocompatibility complex loci. Genetics 124: 967–978.
4. Takahata N (1990) A simple genealogical structure of strongly balanced allelic lines and trans-species evolution of polymorphism. Proc Natl Acad Sci U S A 87: 2419–2423.
5. Hughes AL, Nei M (1988) Pattern of nucleotide substitution at major histocompatibility complex class I loci reveals overdominant selection. Nature 335: 167–170.
6. Hughes AL, Nei M (1989) Nucleotide substitution at major histocompatibility complex class II loci: evidence for overdominant selection. Proc Natl Acad Sci U S A 86: 958–962.
7. Klein J (1987) Origin of major histocompatibility complex polymorphism: the trans-species hypothesis. Hum Immunol 19: 155–162.
8. Hedrick PW, Thomson G (1983) Evidence for balancing selection at HLA. Genetics 104: 449–456.
9. Solberg OD, Mack SJ, Lancaster AK, Single RM, Tsai Y, et al. (2008) Balancing selection and heterogeneity across the classical human leukocyte antigen loci: a meta-analytic review of 497 population studies. Hum Immunol 69: 443–464.
10. Aly TA, Eller E, Ide A, Gowan K, Babu SR, et al. (2006) Multi-SNP analysis of MHC region: remarkable conservation of HLA-A1-B8-DR3 haplotype. Diabetes 55: 1265–1269.
11. Horton R, Gibson R, Coggill P, Miretti M, Allcock RJ, et al. (2008) Variation analysis and gene annotation of eight MHC haplotypes: the MHC Haplotype Project. Immunogenetics 60: 1–18.
12. Alper CA, Larsen CE, Dubey DP, Awdeh ZL, Fici DA, et al. (2006) The haplotype structure of the human major histocompatibility complex. Hum Immunol 67: 73–84.
13. Yunis EJ, Larsen CE, Fernandez-Vina M, Awdeh ZL, Romero T, et al. (2003) Inheritable variable sizes of DNA stretches in the human MHC: conserved extended haplotypes and their fragments or blocks. Tissue Antigens 62: 1–20.
14. Traherne JA, Horton R, Roberts AN, Miretti MM, Hurles ME, et al. (2006) Genetic analysis of completely sequenced disease-associated MHC haplotypes identifies shuffling of segments in recent human history. PLoS Genet 2: e9.
15. de Bakker PI, McVean G, Sabeti PC, Miretti MM, Green T, et al. (2006) A high-resolution HLA and SNP haplotype map for disease association studies in the extended human MHC. Nature genetics 38: 1166–1172.
16. Awdeh ZL, Raum D, Yunis EJ, Alper CA (1983) Extended HLA/complement allele haplotypes: evidence for T/t-like complex in man. Proc Natl Acad Sci U S A 80: 259–263.
17. Sabeti PC, Reich DE, Higgins JM, Levine HZ, Richter DJ, et al. (2002) Detecting recent positive selection in the human genome from haplotype structure. Nature 419: 832–837.
18. Ohashi J, Naka I, Patarapotikul J, Hananantachai H, Brittenham G, et al. (2004) Extended linkage disequilibrium surrounding the hemoglobin E variant due to malarial selection. Am J Hum Genet 74: 1198–1208.
19. Ewens WJ (1972) The sampling theory of selectively neutral alleles. Theor Popul Biol 3: 87–112.
20. Excoffier L, Slatkin M (1995) Maximum-likelihood estimation of molecular haplotype frequencies in a diploid population. Mol Biol Evol 12: 921–927.
21. Lewontin RC (1964) The Interaction of Selection and Linkage. I. General Considerations; Heterotic Models. Genetics 49: 49–67.
22. Mitsunaga S, Kuwata S, Tokunaga K, Uchikawa C, Takahashi K, et al. (1992) Family study on HLA-DPB1 polymorphism: linkage analysis with HLA-DR/DQ and two "new" alleles. Human immunology 34: 203–211.

23. Cullen M, Erlich H, Klitz W, Carrington M (1995) Molecular mapping of a recombination hotspot located in the second intron of the human TAP2 locus. American journal of human genetics 56: 1350–1358.
24. Djilali-Saiah I, Benini V, Daniel S, Assan R, Bach JF, et al. (1996) Linkage disequilibrium between HLA class II (DR, DQ, DP) and antigen processing (LMP, TAP, DM) genes of the major histocompatibility complex. Tissue antigens 48: 87–92.
25. Stephens M, Scheet P (2005) Accounting for decay of linkage disequilibrium in haplotype inference and missing-data imputation. Am J Hum Genet 76: 449–462.
26. Stephens M, Smith NJ, Donnelly P (2001) A new statistical method for haplotype reconstruction from population data. Am J Hum Genet 68: 978–989.
27. Miretti MM, Walsh EC, Ke X, Delgado M, Griffiths M, et al. (2005) A high-resolution linkage-disequilibrium map of the human major histocompatibility complex and first generation of tag single-nucleotide polymorphisms. Am J Hum Genet 76: 634–646.
28. Gonzalez-Galarza FF, Christmas S, Middleton D, Jones AR (2011) Allele frequency net: a database and online repository for immune gene frequencies in worldwide populations. Nucleic Acids Res 39: D913–919.
29. Abdulla MA, Ahmed I, Assawamakin A, Bhak J, Brahmachari SK, et al. (2009) Mapping human genetic diversity in Asia. Science 326: 1541–1545.
30. Gjesing AP, Andersen G, Burgdorf KS, Borch-Johnsen K, Jorgensen T, et al. (2007) Studies of the associations between functional beta2-adrenergic receptor variants and obesity, hypertension and type 2 diabetes in 7,808 white subjects. Diabetologia 50: 563–568.
31. Song EY, Park MH, Kang SJ, Park HJ, Kim BC, et al. (2002) HLA class II allele and haplotype frequencies in Koreans based on 107 families. Tissue Antigens 59: 475–486.
32. Ohashi J, Naka I, Tsuchiya N (2011) The impact of natural selection on an ABCC11 SNP determining earwax type. Mol Biol Evol 28: 849–857.
33. Tishkoff SA, Varkonyi R, Cahinhinan N, Abbes S, Argyropoulos G, et al. (2001) Haplotype diversity and linkage disequilibrium at human G6PD: recent origin of alleles that confer malarial resistance. Science 293: 455–462.
34. Blackwell JM, Jamieson SE, Burgner D (2009) HLA and infectious diseases. Clin Microbiol Rev 22: 370–385, Table of Contents.
35. Kamatani Y, Wattanapokayakit S, Ochi H, Kawaguchi T, Takahashi A, et al. (2009) A genome-wide association study identifies variants in the HLA-DP locus associated with chronic hepatitis B in Asians. Nat Genet 41: 591–595.
36. Voight BF, Kudaravalli S, Wen X, Pritchard JK (2006) A map of recent positive selection in the human genome. PLoS Biol 4: e72.
37. Dunbar SA (2006) Applications of Luminex xMAP technology for rapid, high-throughput multiplexed nucleic acid detection. Clin Chim Acta 363: 71–82.
38. Rousset F (2008) genepop'007: a complete re-implementation of the genepop software for Windows and Linux. Mol Ecol Resour 8: 103–106.
39. Excoffier L, Laval G, Schneider S (2005) Arlequin (version 3.0): an integrated software package for population genetics data analysis. Evol Bioinform Online 1: 47–50.
40. Watterson GA (1978) The homozygosity test of neutrality. Genetics 88: 405–417.
41. Martin M, Mann D, Carrington M (1995) Recombination rates across the HLA complex: use of microsatellites as a rapid screen for recombinant chromosomes. Hum Mol Genet 4: 423–428.
42. Begovich AB, McClure GR, Suraj VC, Helmuth RC, Fildes N, et al. (1992) Polymorphism, recombination, and linkage disequilibrium within the HLA class II region. J Immunol 148: 249–258.

JVI Journals.ASM.org

Novel Cell Culture-Adapted Genotype 2a Hepatitis C Virus Infectious Clone

Tomoko Date,[a] Takanobu Kato,[a] Junko Kato,[b] Hitoshi Takahashi,[a]* Kenichi Morikawa,[a,c]* Daisuke Akazawa,[a,d] Asako Murayama,[a] Keiko Tanaka-Kaneko,[e] Tetsutaro Sata,[e]* Yasuhito Tanaka,[f] Masashi Mizokami,[g] and Takaji Wakita[a]

Department of Virology II, National Institute of Infectious Diseases, Tokyo,[a] Institute of Geriatrics, Tokyo Women's Medical University, Tokyo,[b] Division of Gastroenterology, Department of Medicine, Showa University School of Medicine, Tokyo,[c] Pharmaceutical Research Laboratories, Toray Industries, Inc., Kanagawa,[d] Department of Pathology, National Institute of Infectious Diseases, Tokyo,[e] Department of Virology and Liver Unit, Nagoya City University Graduate School of Medical Sciences, Nagoya,[f] and The Research Center for Hepatitis and Immunology, National Center for Global Health and Medicine, Chiba,[g] Japan

Although the recently developed infectious hepatitis C virus system that uses the JFH-1 clone enables the study of whole HCV viral life cycles, limited particular HCV strains have been available with the system. In this study, we isolated another genotype 2a HCV cDNA, the JFH-2 strain, from a patient with fulminant hepatitis. JFH-2 subgenomic replicons were constructed. HuH-7 cells transfected with *in vitro* transcribed replicon RNAs were cultured with G418, and selected colonies were isolated and expanded. From sequencing analysis of the replicon genome, several mutations were found. Some of the mutations enhanced JFH-2 replication; the 2217AS mutation in the NS5A interferon sensitivity-determining region exhibited the strongest adaptive effect. Interestingly, a full-length chimeric or wild-type JFH-2 genome with the adaptive mutation could replicate in Huh-7.5.1 cells and produce infectious virus after extensive passages of the virus genome-replicating cells. Virus infection efficiency was sufficient for autonomous virus propagation in cultured cells. Additional mutations were identified in the infectious virus genome. Interestingly, full-length viral RNA synthesized from the cDNA clone with these adaptive mutations was infectious for cultured cells. This approach may be applicable for the establishment of new infectious HCV clones.

Hepatitis C virus (HCV) is a principal agent in posttransfusion and sporadic acute hepatitis (6, 19). HCV belongs to the *Flaviviridae* family and *Hepacivirus* genus. Infection with HCV leads to chronic liver diseases, including cirrhosis and hepatocellular carcinoma (16). HCV is a major public health problem, infecting an estimated 170 million people worldwide (6, 16, 19). Current standard therapy for HCV-related chronic hepatitis is based on the combination of interferon (IFN) and ribavirin although virus eradication rates are limited to around 50% (7, 24, 30). Telaprevir and boceprevir were approved by the U.S. Food and Drug Administration in 2011 in combination with pegylated alpha interferon and ribavirin for the treatment of genotype 1 chronic hepatitis C (34, 35). Both agents inhibit the NS3-NS4A serine protease essential for replication of HCV (25, 36). It is important to develop more anti-HCV drugs with different modes of action to achieve greater efficacy and to avoid the emergence of drug-resistant viruses. To that end, a detailed understanding of the viral replication mechanism is needed to discover novel antiviral targets. An efficient virus culture system is indispensable for detailed analysis of HCV life cycles. In an important development, a subgenomic HCV RNA replicon system has been developed (22) to assess HCV replication in cultured cells. Furthermore, an efficient HCV culture system was established by using a JFH-1 strain virus isolated from a fulminant hepatitis patient (20, 38, 41). By transfection of *in vitro* transcribed full-length JFH-1 HCV RNA into HuH-7 cells, efficient JFH-1 RNA replication and infectious viral particle production were detected. However, this efficient virus production was not reproduced by other HCV strains, even when adaptive mutations were introduced to enhance the replication efficiency in cultured cells (29). Thus, other HCV strains that can replicate in cultured cells and produce infectious virus particles are needed. The J6CF strain is infectious to chimpanzees but does not replicate in cultured cells (26, 27, 40). We constructed chimeric replicon and virus constructs of the J6CF and JFH-1 strains to elucidate the difference in their molecular mechanisms (26, 27). We determined that the NS3 helicase and the NS5B to 3′X regions are important for the efficient replication of the JFH-1 strain and that several amino acid mutations in the C terminus of NS5B are pivotal for replication. However, we could not rescue the replication of other virus strains, such as Con1, with these mutations. This result indicates that different approaches are needed to create replication-competent virus strains in cultured cells.

In the present study, we isolated HCV cDNA, named JFH-2, from a fulminant hepatitis patient. The replication efficiency of the JFH-2 clone in the subgenomic replicon assay was lower than that of JFH-1 although the introduction of adaptive mutations enhanced JFH-2 replication. Interestingly, the full-length chimeric or wild-type JFH-2 genome with adaptive mutations could replicate and produce infectious virus particles. The virus infection efficiency was sufficient for autonomous virus propagation in cultured cells.

MATERIALS AND METHODS

Cell culture system. HuH-7, Huh-7.5.1 (a generous gift from Francis V. Chisari), and Huh7-25 cells were cultured in 5% CO_2 at 37°C in Dulbec-

Received 29 December 2011 **Accepted** 2 July 2012
Published ahead of print 11 July 2012
Address correspondence to Takaji Wakita, wakita@nih.go.jp.
* Present address: Hitoshi Takahashi, Influenza Virus Research Center, National Institute of Infectious Diseases, Musashimurayama, Tokyo, Japan; Kenichi Morikawa, Division of Gastroenterology and Hepatology, Centre Hospitalier Universitaire Vaudois, University of Lausanne, Lausanne, Switzerland; Tetsutaro Sata, Toyama Institute of Health, Toyama, Japan.

doi:10.1128/JVI.07233-11

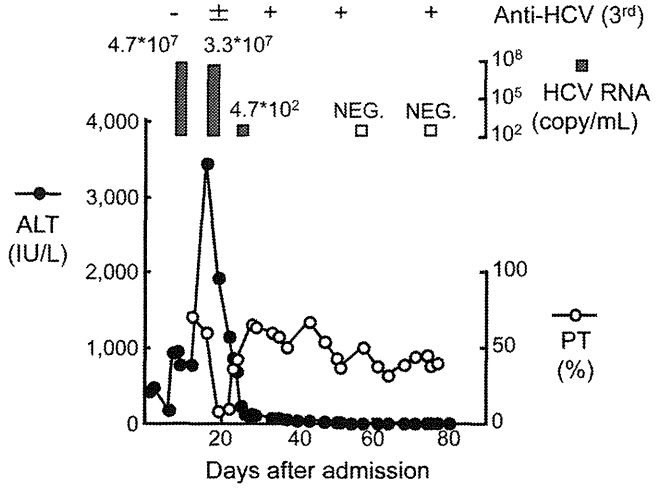

FIG 1 Clinical course of second fulminant hepatitis patient infected with JFH-2. The patient was admitted by reason of acute liver failure. Alanine aminotransferase (ALT) levels, prothrombin time (PT), HCV RNA, and anti-HCV antibodies were determined and followed in his serum.

co's modified Eagle's medium (DMEM) containing 10% fetal bovine serum (DMEM-10) (3, 41).

HCV clones. The genotype 2a clone JFH-2 was isolated from a patient with fulminant hepatitis (15). Briefly, HCV cDNA was cloned from a fulminant hepatitis patient, a 62-year-old man who had a history of coronary artery bypass surgery without blood transfusion. One year after the surgery, he developed an acute auditory disorder and received a course of betamethasone therapy. After withdrawal of betamethasone, the patient developed fulminant hepatitis as diagnosed by acute liver failure associated with stage II encephalopathy and low prothrombin time. He experienced prolonged liver failure and died after 80 days. HCV RNA was detected in his serum only during the acute phase (Fig. 1). Total RNA was extracted from serum during the acute phase, and HCV cDNA covering the entire genome was amplified by reverse transcription-PCR (RT-PCR). All amplified products were purified and then cloned into pGEM-T EASY vectors (Promega, Madison, WI). PCR products and plasmids were sequenced by using specific primer sets (Table 1), BigDye Terminator Mix, and an automated DNA sequencer (models 310 and 377; PE Biosystems, Foster City, CA). The JFH-2 subgenomic replicon (SGR) clones, pSGR-JFH2.1 and pSGR-JFH2.2 (DDBJ/EMBL/GenBank accession numbers AB690456 and AB690457, respectively), were constructed according to the method for pSGR-JFH1 construction (11). Several mutations were introduced into the pSGR-JFH2.1 replicon construct, as reported previously (11). The reporter replicon constructs, pSGR-JFH2.1/Luc and pSGR-JFH2.1/Luc, were developed by rearrangement with pSGR-JFH2.1 and pSGR-JFH2.2 (accession numbers AB690458 and AB690459, respectively) as described previously (12). pJ6/JFH1 was previously obtained from pJFH1 by replacement with the 5′ untranslated region (UTR) to the p7 region (EcoRI-BclI) of the J6CF strain (a kind gift from Jens Bukh) (3, 40). A full-length HCV cDNA was constructed by using the 5′ end to NS2 of pJ6/JFH1 and NS3 to the 3′ end of pSGR-JFH2.1, and the resulting construct was named pJ6/JFH2 (accession number AB690460). Another full-length HCV construct, pJFH2 containing the full-length JFH-2 cDNA downstream of the T7 RNA promoter sequence, was also constructed by replacing the 5′ UTR to NS2 of pJ6/JFH2 with JFH2 sequences, as described previously (accession number AB690461) (1, 37, 38).

Subgenomic replicon assay. Subgenomic replicon RNA was synthesized as reported previously (11). Synthesized replicon RNA was adjusted to 10 μg with cellular RNA isolated from untransfected HuH-7 cells and then electroporated into naive HuH-7 cells as reported previously (11). G418 (1.0 mg/ml) was added to the culture medium, and the drug-resistant colonies were fixed with buffered formalin and stained with crystal violet or cloned and expanded for further analysis. Total RNA was extracted from the cloned G418-resistant cells by using Isogen reagent (Nip-

TABLE 1 Primer list used for cloning and sequencing of JFH-2 clone

Forward primer		Reverse primer	
Name	Sequence (5′→3′)	Name	Sequence (5′→3′)
44S	CTGTGAGGAACTACTGTCTT	1323R	GGTGACCAGTTCATCATCAT
317S	GGGAGGTCTCGTAGACCGTG	1440R	GCTCCCTGCATAGAGAAGTA
844S	GGGTTAATTATGCAACAGGGAAC	2367R	CATTCCGTGGTAGAGTGCA
1141S	TGTCCGCCACGCTCTGCT	2445R	TCCACGATGTTTTGGTGGAG
1361S	CCCGAGGTCATCATAGACAT	3568R	TGTTCCGAGGAAGGACTGAG
2106S	CTGTTGTGCCCCACGGACTG	3765R	TCAGCGTTCCGCGTGACCA
2285S	AACTTCACTCGTGGGGATCG	4706R	TTGCAGTCGATCACGGAGTC
3211S	GGCACTTACATCTATGACCACCTC	5331R	GAGGTCATGACCAGCACGTG
3471S	TGGGCACCATAGTGGTGAG	5563R	CTGCAGCAAGCCTTGGATCT
3930S	TCGATTTCATCCCCGTTGAG	5970R	TTCTCGCCAGACATGATCTT
4278S	CCTATGACATCATCATATGCGATGAATGCC	6152R	AGTGAGTAGGGGCGACGTGGTTTCCTCTGG
4301S	CCTATGACATCATCATATGCGATG	6505R	CCTGCCAGGTGTTCATGCAG
4547S	AAGTGTGACGAGCTCGCGG	6605R	GCATACTCTGAGGCCGCCAC
5021S	TTTTGGGAGGCAGTTTTCAC	6897R	GTGATGTGGGGCGGATCTGTTAGCATGGAC
6383S	TGTCAAAAGGGGTACAAGGG	7648R	TCCTCCTCGGAGCAAGTAGA
6774S	TCCGGGATGAGGTCTCGTTC	8913R	GCGTACTGGATGATGTTTCC
6881S	ATTGATGTCCATGCTAACAG	3X-54R	GCGGCTCACGGACCTTTCAC
7198S	GGCTTGGGCACGGCCTGA	3X-75R	TACGGCACTCTCTGCAGTCA
7244S	ACCGCTTGTGGAATCGTGGA		
7657S	CGTGTGCTGCTCCATGTCAT		
7993S	CAGCTTGTCCGGGAGGGC		
8337S	TTTCGTATGATACCCGATGCTT		
8704S	CGCCCCTCCGGGTGACCCCCCCAGACCGGA		
9123S	CACGAACTGACGCGGGTGGC		

pon Gene, Tokyo, Japan), and the replicon RNA was quantitated by Northern blotting and real-time detection RT-PCR as reported previously (11, 37). The cDNAs of the HCV RNA replicon were synthesized and then amplified by PCR. The sequence of each replicon was determined.

Luciferase reporter replicons were analyzed as follows. Five micrograms of synthesized replicon RNA was transfected into HuH-7 cells by electroporation. Transfected cells were harvested serially at 4, 24, 48, 72, and 96 h after transfection. Luciferase activities were quantified by a Lumat LB9507 instrument (EG&G Berthold, Bad Wildbad, Germany) and a luciferase assay system (Promega). Assays were performed at least in triplicate, and the results were expressed as relative luciferase activity.

Analysis of G418-resistant cells. In RNA-transfected dishes, G418-resistant colonies were isolated by using a cloning cylinder (Asahi Techno Glass Co., Tokyo, Japan) and expanded until 80% to 90% confluence in 10-cm diameter dishes. Expanded cells were analyzed as described previously (11).

Northern blot analysis. Four micrograms of isolated RNA samples was electrophoretically separated in a 1% agarose gel containing formaldehyde and transferred to a positively charged nylon membrane (Hybond-N+; GE Healthcare UK, Ltd., Buckinghamshire, England) and immobilized by a Stratalinker UV cross-linker (Stratagene, La Jolla, CA). Hybridization was performed with a [α-^{32}P]dCTP-labeled DNA probe by using Rapid-Hyb Buffer (GE Healthcare UK, Ltd.). The NS3 to 3′X region of the JFH-1 sequence was used as a template of DNA probe synthesis with a Megaprime DNA Labeling System (GE Healthcare UK, Ltd.) (37).

Western blot analysis of HCV proteins. The protein samples were separated on a 10% polyacrylamide gel. After electrophoresis, the proteins were transferred to a polyvinylidene difluoride membrane (Immobilon; Millipore Corp., Bedford, MA) with a semidry blotting apparatus (Biocraft, Tokyo, Japan). Transferred proteins were incubated with blocking buffer containing 5% nonfat dry milk (Snow brand, Sapporo, Japan) in phosphate-buffered saline. Anti-NS3 rabbit polyclonal antibody raised against recombinant NS3 protein and horseradish peroxidase-labeled goat anti-rabbit Ig (BioSource, Camarillo, CA) were used to detect HCV NS3 protein. The signals were detected with a chemiluminescence system (ECL Plus; GE Healthcare UK, Ltd.). The quantity and quality of the loaded samples were confirmed to be similar by Coomassie brilliant blue staining of the gel.

RT-PCR and sequencing analysis. The cDNAs of HCV RNA were synthesized from total cellular RNA isolated from replicon RNA-transfected cells or from the culture medium of full-length HCV RNA-transfected cells with antisense primer in the 3′X tail region. These cDNAs were subsequently amplified with DNA polymerase (TaKaRa LA Taq; TaKaRa Bio Inc.). The sequence of each amplified DNA was determined directly as described above.

Full-length HCV RNA transfection. Full-length HCV RNA was synthesized from pJ6/JFH2, pJFH2, and the derivatives of these constructs with adaptive mutations, as described previously (13, 37, 38). Synthesized HCV RNA (10 μg) was transfected into Huh-7.5.1 or Huh7-25 cells. HCV core protein levels in the culture medium were measured by immunoassay (31). HCV RNA levels in the culture medium were quantified as described above. Infectivity of culture supernatants was determined by measuring the focus formation efficiency (13, 41). In some experiments, HCV core protein levels in the transfected cells were determined as described previously (37, 38). To examine virus secretion and infectivity after long-term culture, the transfected cells were serially passaged. Virus infection was neutralized by using mouse anti-CD81 monoclonal antibody (clone JS-81; BD Pharmingen, Franklin Lakes, NJ) and anti-HCV human IgG purified from HCV carrier serum (a gift from H. Yoshizawa and J. Tanaka, Hiroshima University).

Density gradient analysis. Culture medium derived from the transfected or infected cells was harvested for density gradient analysis. Cleared culture medium was layered onto a stepwise sucrose gradient (60% [wt/vol] to 10%) and centrifuged for 16 h in an SW41 rotor (Beckman, Palo Alto, CA) at 200,000 $\times$ *g* at 4°C. After centrifugation, 18 fractions were harvested from the bottom of the tubes. The HCV core protein, HCV RNA levels, and infectivity in each fraction were determined as described above.

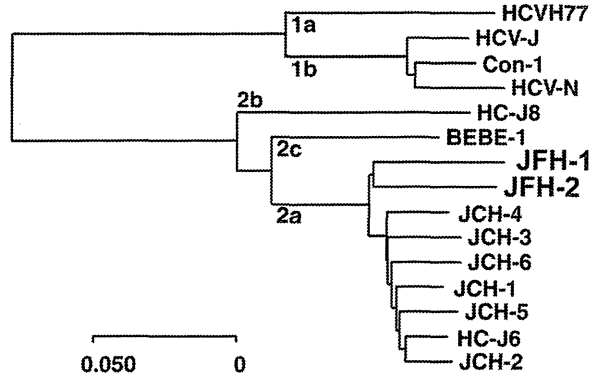

FIG 2 Phylogenetic analysis of JFH-2. Phylogenetic tree of the NS3 to NS5B amino acid sequences of HCV including the JFH-2 strain and genotype 2 strains for which the entire genome has been reported (JFH-1, accession number AB047639; HC-J6, D00944; HC-J8, D10988; and BEBE1, D50409) and representative genotype 1 strains for which the entire genome has been reported (H77, AF009606; HCV-Con1, AJ238799; HCV-J, D90208, and HCV-N, AF139594). This phylogenetic tree was drawn by using Kimura's two-parameter method.

Electron microscopy. To visualize HCV particles, we adsorbed the density gradient-purified virus samples onto carbon-coated grids for 1 min. Then, the grids were stained with 1% uranyl acetate for 1 min and examined under an H-7650 transmission electron microscope (Hitachi High-Technologies Co., Tokyo, Japan) (32). Immunogold labeling was performed with an antibody directed against E2 (AP33; a kind gift from Genentech, South San Francisco, CA) diluted 1:50 in blocking solution and secondary antibody coupled to 10-nm gold particles.

Human hepatocyte chimeric mouse experiments. Human hepatocytes were transplanted into urokinase-type plasminogen activator-transgenic SCID mice(uPA$^{+/+}$ SCID$^{+/+}$) as described previously (33). All mice received hepatocyte transplants from the same donor. Human hepatocyte chimeric mice, in which liver cells were largely (>90%) replaced with human hepatocytes, were used to reduce the potential influence by mouse-derived mRNA. Human albumin levels in the sera of mice were monitored to evaluate the replacement ratio of the human hepatocytes in the mouse liver. The mice were obtained from Phoenix Bio Co., Ltd. (Hiroshima, Japan). Four mice were divided into two groups. Each group of mice was inoculated with 1×10^6 RNA copies of either purified J6/JFH2/AS HCV particles or JFH-2 patient serum. The HCV RNA titer in inoculated mouse serum was monitored by real-time detection RT-PCR each week after inoculation.

RESULTS

HCV clone from a fulminant hepatitis patient. HCV cDNA was isolated from a fulminant hepatitis patient as described in Materials and Methods (clone JFH-2) (15). HCV RNA was detected by RT-PCR in the patient's serum during the acute phase (Fig. 1). All viral markers of the other hepatitis viruses were negative. By the phylogenetic analysis, the JFH-2 clone was clustered into genotype 2a (Fig. 2). JFH-2 exhibits 87.6%, 89.0%, and 88.9% nucleotide homology with JFH-1, J6CF, and JCH-1, respectively, and 90.6%, 91.8%, and 91.8% amino acid homology with JFH-1, J6CF, and JCH-1, respectively (Table 2). The JFH-1 strain is cell culture replication-competent, but the J6CF and JCH-1 strains are incompetent. However, the homology data for nucleotide and amino acid sequences are very similar in both the structural and nonstructural regions. We also mapped the

TABLE 2 Percent homology between JFH-2 and other genotype 2a strains

Region	JFH-2 nucleotide profile				JFH-2 amino acid profie			
	Lenght (nt)[a]	% Identity vs strain:			Length (aa)[b]	% Amino acid identity vs strain:		
		JFH-1	J6CF	JCH-1		JFH-1	J6CF	JCH-1
Entire genome	9683	87.60	88.98	88.88	3033	90.64	91.79	91.79
UTR[c]	576	96.35	98.61	96.88	NA[d]			
Structural	2439	86.14	87.90	86.51	813	89.30	89.54	88.56
Nonstructural	6663	87.44	88.59	89.12	2220	91.13	92.61	92.97
5′ UTR	340	98.82	99.71	99.71	NA			
Core	573	91.80	93.02	91.97	191	92.15	95.29	92.15
E1	576	87.50	88.89	89.06	192	90.10	92.19	89.58
E2-p7	1290	83.02	85.19	82.95	430	87.67	85.81	86.51
NS2	651	84.18	85.87	89.09	217	87.56	88.02	91.24
NS3	1893	87.64	88.54	89.33	631	92.87	94.61	94.45
NS4A	162	88.27	88.27	88.27	54	96.30	92.59	94.44
NS4B	783	89.91	90.04	89.14	261	96.93	97.32	96.55
NS5A	1398	83.48	85.98	85.48	466	82.83	86.70	86.48
NS5B	1776	90.37	91.10	91.84	591	94.08	94.75	95.43
3′ UTR	236	92.80	97.03	92.80	NA			

[a] nt, nucleotides.
[b] aa, amino acids.
[c] UTR, 5′ UTR plus 3′ UTR.
[d] NA, not applicable.

positions of different amino acid sequences of each strain (Fig. 3A). The E2 and NS5A regions are more variable than other regions (Fig. 3A and Table 2); however, it is difficult to find particular mutation positions or regions specific for the JFH-2 strain.

Subgenomic replicon analysis of the JFH-2 clone. Interestingly, some parts of the viral cDNA sequences in the JFH-2 viral genome were a mixture of different sequences, especially in the NS3 region. By the cloning analysis, we found two major se-

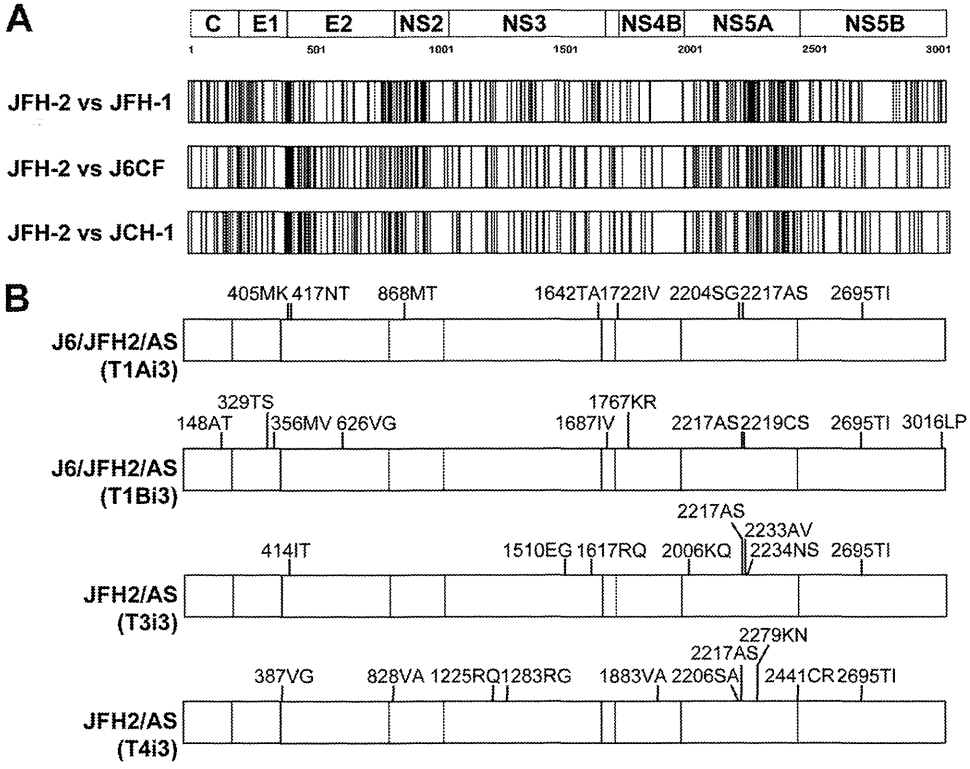

FIG 3 Maps of amino acid sequences among genotype 2a HCV strains and mutations found in the cell culture-adapted viruses. (A) Amino acid sequences of the entire open reading frame (3,033 amino acids) of JFH-1, JFH-2, J6CF (accession numbers AB047639, AB690461, and AF177036, respectively), and JCH-1 strains were compared. The positions of different sequences are indicated by vertical lines. (B) Virus genome sequences were determined in the T1Ai3 and T1Bi3 culture media of the J6/JFH2/AS virus-inoculated cells or T3i3 and T4i3 culture media of the JFH2/AS virus-inoculated cells, as described in the text. Amino acid mutations are indicated with their positions and residues.

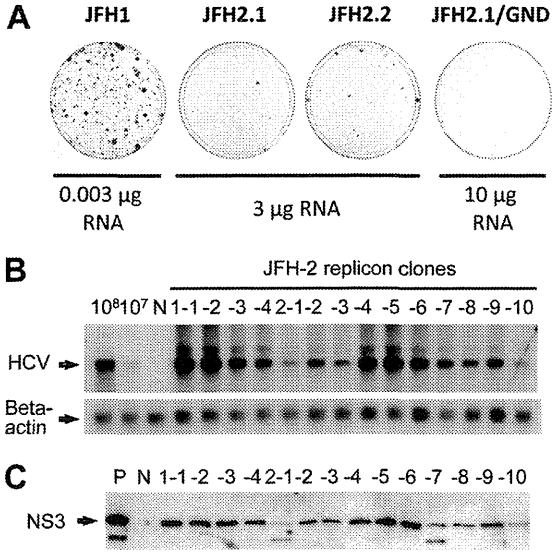

FIG 4 G418-resistant colony formation of JFH-1 and JFH-2 replicons and analysis of JFH-2 replicon cells. (A) Subgenomic RNAs were synthesized *in vitro* by using pSGR-JFH1, pSGR-JFH2.1, pSGR-JFH2.2, and pSGR-JFH2.1/GND as templates. Transcribed subgenomic RNAs were electroporated into HuH-7 cells, and cells were cultured with G418 for 3 weeks before being stained with crystal violet. JFH-1 subgenomic RNA (0.003 μg), 3 μg of JFH-2.1 and JFH-2.2 subgenomic RNA, and 10 μg of JFH-2.1/GND subgenomic RNA were transfected into HuH-7 cells. Experiments were performed in triplicate, and representative staining examples are shown. (B) Northern blot analysis. Total cellular RNA isolated from each of four SGR-JFH2.1 clones (1-1 to 1-4) and 10 SGR-JFH2.2 clones (2-1 to 2-10) was analyzed by using a random-primed DNA probe to detect replicon RNA. Isolated total cellular RNA (4 μg) was separated by denatured agarose gel electrophoresis. After electrophoresis, HCV- and beta-actin-specific RNAs were detected by Northern blot analysis with random-primed DNA probes specific to HCV and beta-actin sequences. Arrows indicate replicon RNA or beta-actin mRNA. (C) Western blot analysis. Cell lysates were prepared from four SGR-JFH2.1 clones (1-1 to 1-4) and 10 SGR-JFH2.2 clones (2-1 to 2-10). The NS3 proteins were detected with rabbit anti-HCV NS3 antibody. Positive-control (P) and negative-control (N) cell lysates were obtained from JFH-1 replicon cells and naive HuH-7 cells.

quences in the JFH-2 viral genome. One sequence contained alanine and isoleucine (AI) at amino acid positions 1204 and 1205, and the other contained methionine and leucine (ML) at the same positions. We referred to these viral genomes containing AI or ML as JFH-2.1 or JFH-2.2, respectively. From the cloning analysis of PCR products, JFH-2.1 populated 19 of 32 clones (59%), and JFH-2.2 populated 13 of 32 clones (41%). To analyze the replication efficiency of the JFH-2 clone, we thus constructed two subgenomic replicon constructs, pSGR-JFH2.1 and pSGR-JFH2.2, as pSGR-JFH1 (11). Synthesized replicon RNAs of JFH-2.1 and JFH-2.2 were independently transfected by electroporation into HuH-7 cells. The transfected cells were then grown for 3 weeks in selection culture that contained 1 mg/ml of G418. Several colonies survived the selection culture, as illustrated by crystal violet staining (Fig. 4A). The JFH2.1/GND replication-incompetent control RNA-transfected cells did not form any colonies, even when 10 μg of RNA was transfected. The colony formation efficiencies of the JFH-2.1 and JFH-2.2 replicons were 0.94 ± 0.54 and 6.43 ± 3.39 CFU/μg RNA, respectively, which were substantially lower than the colony formation efficiency of the JFH-1 subgenomic replicon ($5.32 \times 10^4 \pm 5.02 \times 10^4$ CFU/μg RNA) (11). Four colonies of the JFH-2.1 replicon and 10 colonies of the JFH-2.2 replicon were cloned and expanded for further analysis. Replicon RNA was isolated from each replicon cell clone, and the HCV RNA titer and sequence of the replicon genome were determined (Table 3). The average HCV RNA titer in replicon cell clones was determined by real-time RT-PCR detection as $(8.70 \pm 4.94) \times 10^7$ copies/μg of RNA. The size and amount of the replicon RNA in the replicon cells were confirmed by Northern blot analysis (Fig. 4B). We also detected NS3 protein in each clone of replicon cells by Western blot analysis (Fig. 4C). NS3 proteins were mainly found at approximately 70-kDa by polyclonal anti-NS3 antibody; however, an additional signal was also detected at a smaller molecular size in some replicon cells, including the positive-control JFH-1 replicon cells.

Next, we determined the sequences of replicating RNA in each replicon cell clone. Most of the clones, except replicon clone 2.2-8, had at least one nonsynonymous mutation (Table 3). We found nonsynonymous mutations in the NS3, NS5A, and NS5B regions, and three mutations were common among the different replicon genomes. Among the mutations found in the NS3 region, both 1547FL and 1614CW were found in two different replicon cells, and the 1651TN mutation was found in five replicon cells. The 2280QR mutation in NS5A was found in three replicon cells. 2217AS and 2222HQ, which are located in the interferon sensitivity-determining region (ISDR), were each found in a single replicon cell (8). To determine the adaptive effect of these mutations (Fig. 5A), we inserted these mutations (listed in Table 3), except for 1204MK, into pSGR-JFH2.1 and tested the colony formation efficiency of the mutant replicons. The 1204MK mutation was not tested since methionine at amino acid position 1204 was specific for the JFH2.2 sequence. As shown in Fig. 5B, 1547FL, 1614CW, 1651TN, 2222HQ, and 2280QR had weak to moderate adaptive effects for colony formation. Interestingly, the 2217AS mutation in the ISDR strongly enhanced the colony formation to approximately 3×10^4 times that of the parental JFH2.1 replicon (Fig. 5B). We further tested these adaptive mutations in the luciferase reporter replicon format, as described previously (12). SGR-JFH2.1 with the 2217AS construct exhibited significant replication compared to JFH2.1/GND, which is the replication-incompetent negative control. However, other constructs showed no evidence of replication in the transient replication assay (Fig. 5C).

Full-length HCV replication. The 2217AS mutation substantially enhanced RNA replication of the JFH-2.1 subgenomic replicon compared with other mutations. We examined whether a full-length JFH-2 HCV clone with the 2217AS mutation could produce infectious virus. In our previous study, we constructed the J6/JFH1 chimeric construct by replacement of the 5′ untranslated region to the p7 region (EcoRI-BclI) of J6 (1), and we found that J6/JFH1 produces a larger amount of infectious virus in the culture medium (3). We thus used the structural region of the J6CF clone and the NS2 region of the JFH-1 clone from a J6/JFH-1 chimeric virus construct and fused it to the NS3 to 3′X regions of JFH-2.1 with the 2217AS mutation (plasmid pJ6/JFH2/AS) since it was not clear if the structural and NS2 regions of the JFH-2 strain were functionally intact (Fig. 6A). Full-length viral RNA was synthesized from linearized pJ6/JFH2/AS and electroporated into Huh-7.5.1 cells. After two independent transfections, the transfected cells were divided into sub-cell lines to form a total of four sub-cell lines (T1A, T1B, T2A, and T2B). All four sub-cell lines were serially passaged, and HCV core protein, RNA, and infectivity levels in the culture supernatant were monitored (Fig.

TABLE 3 Mutations and RNA titer of the JFH-2 replicon cell clones

Replicon clone	Nucleotide		Amino acid			Replicon titer (no. of copies/μg of RNA)
	Mutation	Position	Mutation	Position	Region	
2.1-1	A→G	2012	E→G	1109	NS3	1.30E+8
	C→A	3638	T→N	1651	NS3	
2.1-2	T→C	3325	F→L	1547	NS3	1.52E+8
	C→A	3638	T→N	1651	NS3	
2.1-3	A→G	5525	Q→R	2280	NS5A	1.09E+8
	A→G	7155	None		NS5B	
2.1-4	C→A	3638	T→N	1651	NS3	1.41E+8
	A→G	7795	None		3′ UTR	
2.2-1	C→G	3528	C→W	1614	NS3	2.33E+7
2.2-2	G→T	5335	A→S	2217	NS5A (ISDR)	3.57E+7
2.2-3	C→G	919	None		*neo*	3.35E+7
	C→A	5352	H→Q	2222	NS5A (ISDR)	
2.2-4	C→A	1223	None		EMCV-IRES[a]	1.05E+8
	C→A	2115	None		NS3	
	G→T	6243	K→N	2519	NS5B	
2.2-5	C→A	3327	F→L	1547	NS3	1.67E+8
2.2-6	T→C	625	None		*neo*	1.09E+8
	C→A	3638	T→N	1651	NS3	
	A→G	5525	Q→R	2280	NS5A	
	T→A	5754	None		NS5A	
	G→A	5803	G→S	2373	NS5A	
2.2-7	C→G	3528	C→W	1614	NS3	6.25E+7
2.2-8	None		None			5.31E+7
2.2-9	C→G	3638	T→N	1651	NS3	6.71E+7
	G→A	5269	A→T	2195	NS5A	
	A→G	5525	Q→R	2280	NS5A	
2.2-10	T→A	2297	M→K	1204	NS3	2.95E+7
	A→G	7815	None		3′ UTR	

[a] EMCV-IRES, encephalomyocarditis virus internal ribosome entry site.

6B and C and Table 4). At the first cell passage, the HCV core protein levels were approximately 300 fmol/liter, and the infectivities were very low. Secreted HCV core protein levels decreased in all of the passaged cells until 25 days after the transfection. However, HCV core protein secretion of passaged T1A cells began to increase from 30 days after transfection. Subsequently, increased core protein secretion was also observed in other passaged cells although at different time points (Fig. 6B and Table 4). The maximum core protein levels in the medium were up to 9,241 fmol/liter in T1B cells at day 75 posttransfection. Infectivity detected in the culture medium was also first increased in T1A, and similar increases were observed with other passaged cells at later time points. Furthermore, specific infectivity (infectivity/HCV RNA or infectivity/HCV core protein) was also higher than in the initial culture medium (Table 4). The passaged cells were immunostained with anti-core monoclonal antibody (Fig. 6D). At 4 weeks after transfection, only a few cells were positive in all four sub-cell lines. However, the number of positive cells increased from 8, 12, 18, or 14 weeks after transfection in T1A, T1B, T2A, or T2B cells, respectively. These results indicate that phenotypic change occurred in the replicating virus after the serial passages of the transfected cells. Before this phenotypic change, the replicating viruses were not able to secrete significant amounts of infectious virus particles due to an unknown defect in infectious virus particle formation or secretion. After the phenotypic change, the robust core protein secretion might have been caused by changes in the efficiency of infectious virus production or secretion. To compare the virus characteristics before and after the phenotypic change, we analyzed T1A culture medium from 5 days, 8 weeks, and 11 weeks posttransfection by density gradient assay (Fig. 6E). The day 5 medium showed a broad density profile both of core protein and HCV RNA, and infectivity was not detected. Interestingly, the peaks of HCV core protein and RNA at around 1.15 mg/ml density became higher at 8 weeks and had a further increase at 11 weeks. Broader minor peaks at the lighter density remained small at week 11. The infectivity peak also became higher at 8 and 11

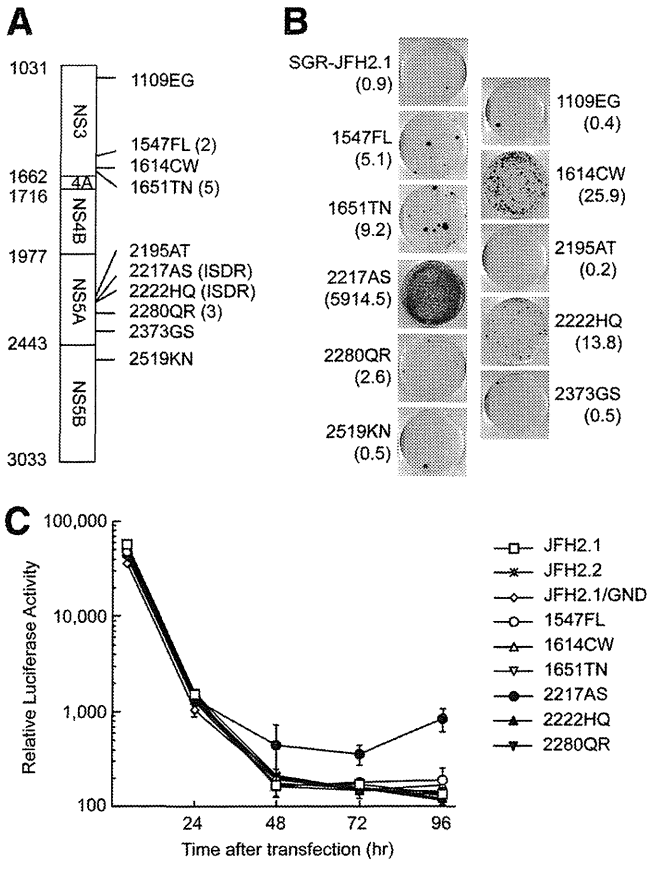

FIG 5 Analysis of the effect on colony formation and transient replication efficiency of mutations detected in replicon cell clones. (A) The box indicates the open reading frame of JFH-2 replicon and amino acid sequences at positions 1031 and 3033 (numbering by full-length JFH-2). The numbers on the left side of the box show the starting position of each protein, with the exception of 3033, which is the end position of NS5B. The numbers with the lines on the right side indicate the mutations introduced in the replicon constructs. 1547FL, 1651TN, and 2280QR mutations were found in 2, 5, and 3 replicon clones, respectively (Table 3). 2217AS and 2222HQ mutations were found in the ISDR (Table 3). (B) Each amino acid mutation found in the replicon genome was introduced into the pSGR-JFH2.1 replicon construct, and colony formation of the JFH2.1 replicon with the wild-type sequence (SGR-JFH2.1) and other mutations was tested. Briefly, transcribed RNA (5 μg) was transfected into HuH-7 cells, and cells were cultured for 3 weeks before being stained with crystal violet. The numbers in the parentheses show the colony formation efficiency (CFU/μg of RNA) of the replicon constructs. (C) Transient replication of JFH-2 subgenomic replicon. HuH-7 cells were transfected with the transcribed RNA from pSGR-JFH2.1/Luc, pSGR-JFH2.2/Luc, pSGR-JFH2.1/Luc/GND (replication-incompetent control), and pSGR-JFH2.1/Luc constructs with adaptive mutations (1547FL, 1614CW, 1651TN, 2217AS, 2222HQ, and 2280QR). Transfected cells were harvested at the indicated time points and at 4 h posttransfection. Relative luciferase activity (arbitrary units) was measured in the cell lysate. Assays were performed in triplicate, and data are presented as means ± standard deviations. The background signal of the luciferase measurement was 129.4 ± 27.4 units.

weeks after transfection. Interestingly, this density profile at 11 weeks posttransfection was quite similar to that of JFH-1 or the J6/JFH1 chimera, as previously described (21, 38). Furthermore, virus-like particles were visualized in the concentrated culture medium by electron microscopic analysis, whereas only unstructured aggregates were found with the mock-transfected control (Fig. 7, left panel; also data not shown). An aliquot of the culture medium was used for immunoelectron microscopy with an E2-specific antibody (AP33), and gold-labeled spherical structures were detected (Fig. 7, middle panel). The overall diameter of the structures (50 to 65 nm) is compatible with the predicted size of HCV.

Characterization of cell culture-adapted J6/JFH2/AS virus. During the serial passages of the transfected cells, the J6/JFH2/AS virus adapted to produce more infectious viruses in the cell culture. We next compared the adapted J6/JFH2/AS virus (T1B cells at day 75 posttransfection) with the J6/JFH1 virus. Huh-7.5.1 cells were inoculated with the viruses at a multiplicity of infection (MOI) of 0.03. The core protein production levels in both the infected cells and the culture medium were increased with similar kinetics after the virus infection, although at lower levels for J6/JFH2/AS virus than J6/JFH1 virus (Fig. 8A). We also tested the neutralization of the infection of these viruses by using mouse anti-CD81 monoclonal antibody and anti-HCV human IgG purified from HCV carrier serum (Fig. 8B). Both antibodies clearly inhibited the infectivity of inoculated virus to Huh-7.5.1 cells. Thus, the J6/JFH2/AS and J6/JFH1 viruses appeared to share similar infection pathways.

Adaptive mutations in the cell culture-adapted J6/JFH2.2/AS virus. We determined the full-length sequence of the HCV genome in the culture medium of T1A and T1B sub-cell lines at 75 days posttransfection by directly sequencing the amplified virus cDNA. We found the following nonsynonymous mutations, in addition to 2217AS, in the viral genomes: 1342ST in NS3 and 2219CR in NS5A of T1A and 148AT in the core protein, 2219CS in NS5A, and 2695TI and 3016LP in NS5B of T1B. These mutations were introduced into the J6/JFH2.2/AS cDNA, and synthetic RNA was transfected into Huh-7.5.1 cells. However, robust virus production was not observed at an early time point after transfection (data not shown). Because the important adaptive mutations might still not be detected in the virus population, we decided to concentrate on the dominant virus population and fix the important mutations in T1A and T1B virus by serial virus passages. We thus repeatedly inoculated naive Huh-7.5.1 cells three times with J6/JFH2/AS virus at a low MOI and harvested the virus when the virus titer plateaued. We sequenced the full-length genome of virus in the culture medium after the third inoculation (T1Ai3 or T1Bi3) and found the following nonsynonymous mutations: 405MK and 417NT in E2, 868MT in NS2, 1642TA in NS3, 1722IV in NS4B, 2204SG in NS5A, and 2695TI in NS5B of T1Ai3; and 148AT in the core protein, 329TS and 356MV in E1, 626VG in E2, 1678IV in NS4A, 1767KR in NS4B, 2219CS in NS5A, and 2695TI and 3016LP in NS5B of T1Bi3 (Fig. 3B). We then introduced these mutations into pJ6/JFH2/AS to construct pJ6/JFH2/AS/mtT1A and pJ6/JFH2/AS/mtT1B. Synthetic RNAs produced from both of the mutation-containing plasmids and control plasmids were transfected into Huh-7.5.1 cells. After the transfection, core proteins were secreted into the culture medium at levels similar to those of JFH-1 RNA-transfected cells but at lower levels than J6/JFH1 RNA-transfected cells (Fig. 9A). HCV RNA levels in the culture medium of J6/JFH2/AS/mtT1A (mtT1A) and J6/JFH2/AS/mtT1B (mtT1B) RNA-transfected cells were less than those in cells transfected with either or JFH-1 J6/JFH1 RNA (Fig. 9B). This discrepancy may be due to the lower detection efficiency of the JFH-1 core protein in the immunoassay, as reported previously (31). Infectivity in the culture medium was also determined. Interestingly, higher infectious titers were detected in the culture medium of the J6/JFH2/AS/mtT1A and J6/JFH2/AS/mtT1B

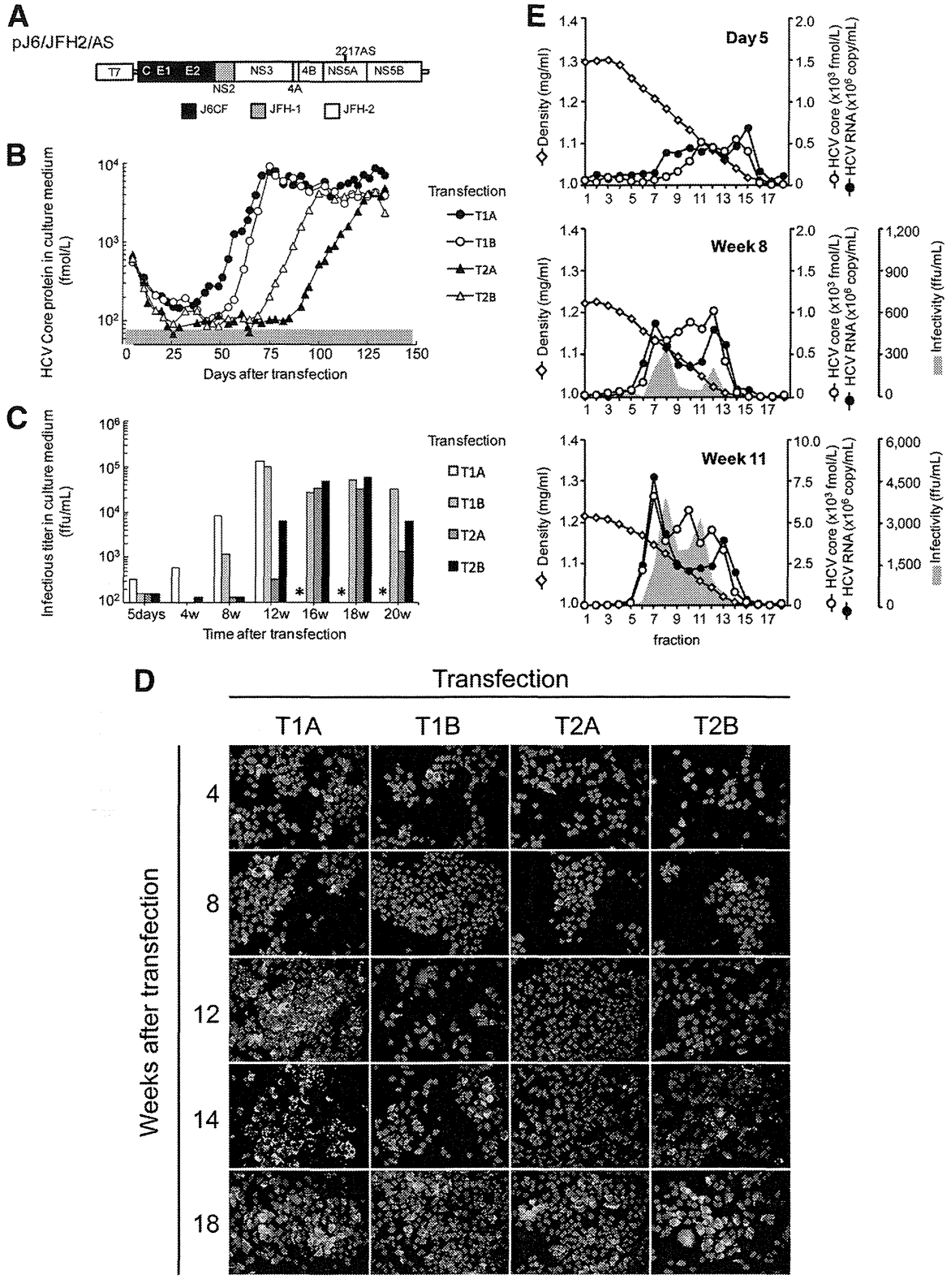

FIG 6 J6/JFH2 chimeric full-length HCV replication. (A) Organization of full-length chimeric JFH-2 construct, pJ6/JFH2/AS. A T7 RNA promoter is located upstream of the 5′ end of the HCV cDNA construct. The 5′ UTR and NS2 region are derived from the JFH-1 strain. Regions of the core protein to E2/p7 are derived from the J6CF strain. The 2217AS adaptive mutation is introduced. (B) Huh-7.5.1 cells were transfected with the transcribed RNA from pJ6/JFH2/AS. Two independently transfected cell lines (transfections 1 and 2 [T1 and T2, respectively]) were divided into two passages, resulting in four independently passaged transfected cell lines (T1A, T1B, T2A, and T2B). At each time point, culture medium was harvested and analyzed for the presence of HCV core protein by Lumipulse Ortho HCV Ag (Ortho-Clinical Diagnostics). The gray area indicates values that are below the detection limit. (C) Infectious titers in the culture supernatant of the passaged transfected cells (T1A, T1B, T2A, and T2B) were determined by focus formation assay. After 16 weeks, the culture media from T1A

TABLE 4 Specific infectivity of culture medium after transfection of J6/JFH2/AS RNA

Cell culture medium (no. of days posttransfection)	Infectivity (FFU/ml)	HCV core protein (fmol/liter)	HCV RNA (no. of copies/ml)	Specific infectivity	
				Infectivity/HCV core protein	Infectivity/HCV RNA (10^4)
T1A (5)	3.20E+1	3.57E+2	2.63E+6	0.09	0.12
T1B (5)	1.60E+1	3.07E+2	2.35E+6	0.05	0.07
T2A (5)	1.60E+1	3.13E+2	2.99E+6	0.05	0.05
T2B (5)	1.60E+1	2.63E+2	3.42E+6	0.06	0.05
T1A (82)	1.28E+4	5.47E+3	2.63E+7	2.34	4.87
T1B (82)	9.83E+3	5.98E+3	2.73E+7	1.64	3.61
T2A (120)	3.17E+3	2.47E+3	8.49E+6	1.28	3.73
T2B (120)	5.83E+3	4.51E+3	2.83E+7	1.29	2.06

RNA-transfected cells than in JFH-1 RNA-transfected cells; however, they were lower than in J6/JFH-1 RNA-transfected cells (Fig. 9C).

Transfected cells were serially passaged, and, importantly, both types of transfected cells (J6/JFH2/AS/mtT1A and J6/JFH2/AS/mtT1B RNA) secreted core protein and HCV RNA at high levels, even at the first passage after transfection, and the levels of HCV core protein and RNA were maintained during the passages (Fig. 10A and B). Infectious titers in the medium of the transfected cells were also measured (Fig. 10C). J6/JFH2/AS/mtT1A secreted a higher infectious titer than J6/JFH2/AS/mtT1B although their HCV core protein levels and RNA levels in the culture medium were similar. To confirm the rapid infectious viral production phenotype of these viruses, we inoculated naive Huh-7.5.1 cells with the culture medium of J6/JFH2/AS/mtT1A and J6/JFH2/AS/mtT1B RNA-transfected cells at 8 and 38 days posttransfection at an MOI of 0.01. All of the inoculated cells secreted core protein and HCV RNA with similar kinetics (Fig. 11A and B). The infectious titer was also determined in the culture medium of the infected and passaged cells (Fig. 11C). mtT1B (day 38 posttransfection) showed lower infectivity at 7 days after inoculation; however, substantial infectivity was detected at 13 and 27 days. The culture medium of mtT1A (day 8 and day 38 posttransfection) was harvested at 20 days after inoculation and analyzed by a sucrose density gradient assay, as described above (Fig. 11D). Major peaks of both HCV core protein and RNA were clearly shown at around 1.15 mg/ml, and the subpeaks of HCV core protein were found in lighter fractions. On the other hand, major peaks of infectivity were found at around 1.0 mg/ml. Compared to the data shown in Fig. 6E, the HCV core and RNA levels and infectivity titer are higher in mtT1A (day 8 and day 38 posttransfection) virus. The similar virus characteristics suggested that J6/JFH2/AS/mtT1A and J6/JFH2/AS/mtT1B viruses do not need further adaptations for autonomous expansion in cultured cells. Thus, we established stable cell culture-adapted virus and constructed recombinant cell culture-adapted infectious HCV clones by reverse genetics.

Human hepatocyte-transplanted uPA/SCID mouse experiment. To determine the *in vivo* infectivity of J6/JFH2/AS virus, we inoculated day 75 culture medium of T1B cells containing 1×10^6 RNA copies of purified J6/JFH2/AS HCV particles and original patient serum also containing 1×10^6 RNA copies into human hepatocyte-transplanted uPA/SCID mice. Inoculation of 1×10^6 RNA copies of cell culture-derived J6/JFH1 virus usually results in robust infection for human hepatocyte-transplanted uPA/SCID mice. Two mice were used for each type of inoculum. Human albumin levels in sera of the inoculated mice were more than 3 mg/ml during the experiment, which supported the high replacement ratio of the human hepatocytes in the mouse liver. Both mice inoculated with patient serum became HCV RNA positive 1 week postinoculation and remained positive during the 4-month observation period (Fig. 12). However, the mice inoculated with J6/JFH2/AS virus in culture medium did not become HCV positive after inoculation (Fig. 12). One mouse inoculated with J6/JFH2/AS virus died 16 days after inoculation, and the cause of death was unknown. HCV RNA was not detected at 7, 14, and 16 days postinoculation. The other mouse inoculated with culture medium was also tested every week for serum HCV RNA and remained negative for 56 days after infection. On day 56, this mouse received a second inoculation with the same culture medium. This mouse was monitored for a total of 63 days, but weekly tests for HCV RNA were continuously negative. Thus, the cell culture-adapted virus in the inoculum may be less viable *in vivo* although the virus acquired robust replication capacity in HuH-7 cells.

Full-length JFH-2 construct. We successfully established J6/JFH2/AS-derived cell culture-adapted viruses. Next, we produced a full-length JFH2/AS virus by using the structural region sequence from JFH-2. pJFH2/AS was constructed according to the viral sequence, and an alanine-to-serine mutation was introduced at amino acid position 2217. JFH2/AS RNA synthesized *in vitro* was electroporated into the Huh-7.5.1 cells, as described above. J6/JFH2/AS RNA was also transfected simultaneously and compared. Two groups of independently transfected cells (transfections 3 and 4 [T3 and T4, respectively]) were analyzed for JFH2/AS and J6/JFH2/AS. Interestingly, JFH2/AS RNA-transfected cells be-

cell lines were not tested (*). (D) The passaged transfected cells were stained with anti-core protein monoclonal antibody (2H9) as a primary antibody at the indicated time points. Green, HCV core protein; blue, 4′,6′-diamidino-2-phenylindole (DAPI) staining. (E) Density gradient analysis of culture supernatant from HCV RNA-transfected Huh-7.5.1 cells. Culture supernatants of transfected cell line T1A collected at 5 days, 8 weeks, and 11 weeks posttransfection were cleared by centrifugation and filtration. Each supernatant was overlaid on the stepwise sucrose density gradient (0%, 10%, 20%, 30%, 40%, 50%, and 60% sucrose) and centrifuged for 16 h at 200,000 × *g* at 4°C. Eighteen fractions were collected from the bottom of the tubes, and the concentration of HCV core protein in each fraction was determined by Lumipulse Ortho HCV Ag. The levels of HCV core protein, HCV RNA, and infectivity were determined in each fraction. Infectivity of the samples from day 5 was negative. Open diamond, buoyant density.

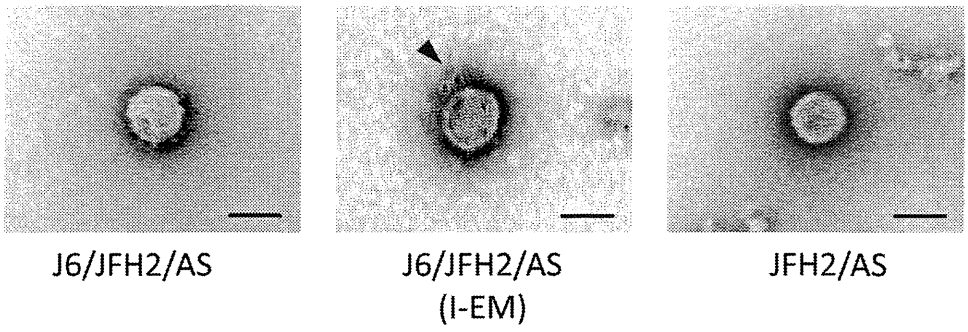

FIG 7 Morphology of JFH-2 virus particles. Negatively stained HCV particles were observed by electron microscopy. J6/JFH-2/AS and JFH2/AS virus particles were purified and observed by electron microscopy by using negative staining. In the middle panel, a J6/JFH-2/AS virus particle was detected by immuno-electron microscopic (I-EM) analysis by using anti-E2 antibody. Arrowhead, gold-labeled antibody. Scale bar, 50 nm.

gan to secrete core proteins earlier than J6/JFH2/AS RNA-transfected cells in this experiment (Fig. 13). Core protein levels were 24,525 and 11,720 fmol/liter in T3 cells at 67 days posttransfection and T4 cells at 63 days posttransfection, respectively. Infectious titers were also determined in the same culture medium at 2.1×10^4 and 4.3×10^4 focus-forming units (FFU)/ml for T3 and T4, respectively. T3 culture medium at day 67 posttransfection was

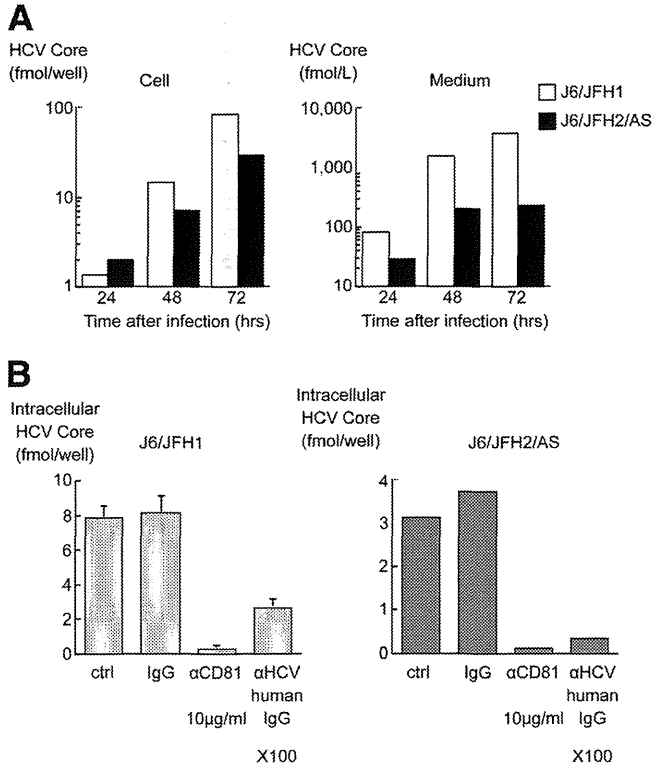

FIG 8 Comparative analysis between J6/JFH1 and J6/JFH2/AS virus. (A) Huh-7.5.1 cells were infected with J6/JFH1 or J6/JFH2/AS virus particles at an MOI of 0.03. HCV core protein production in the inoculated cell lysate and medium was measured at the indicated times. Assays were performed in duplicate, and the average data are represented. (B) Infection with J6/JFH1 and J6/JFH2/AS virus particles was inhibited by adding antibodies to the reaction mixtures. Assays were performed three times independently, and data are presented as means ± standard deviations. Normal human IgG and anti-CD81 monoclonal antibody and anti-HCV human IgG at the indicated concentrations were used. Ctrl, control.

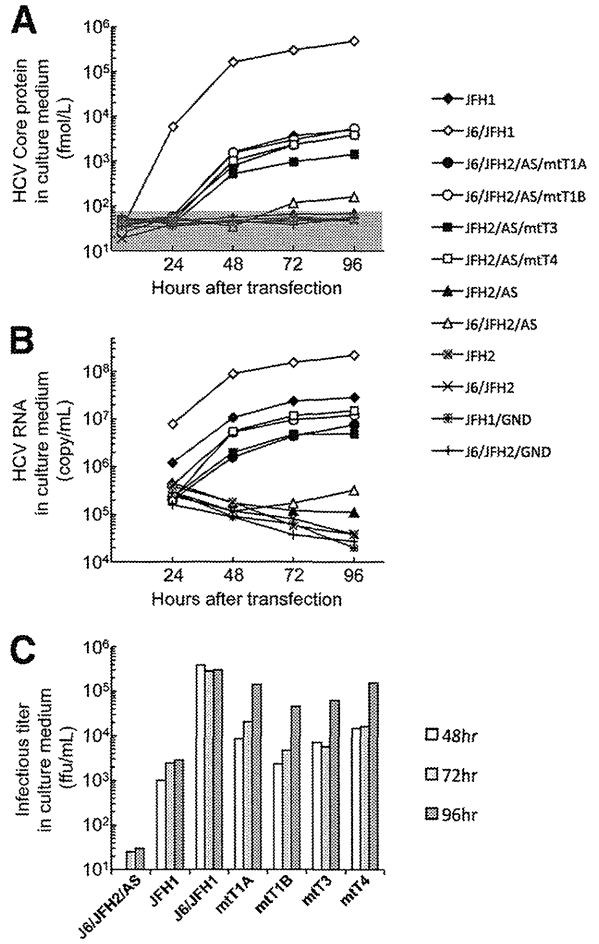

FIG 9 Transient virus production assay of J6/JFH2- and JFH2-related constructs with Huh-7.5.1 cells. Full-length HCV RNA was synthesized from the JFH1, J6/JFH1, JFH2, and J6/JFH2 constructs and their derivatives with mutations and transfected into Huh-7.5.1 cells. (A) HCV core protein levels in the culture medium were determined at 4, 24, 48, 72, and 96 h after transfection. The gray area indicates values that are below the detection limit. (B) HCV RNA levels in the culture medium were also determined at 24, 48, 72, and 96 h after transfection. (C) Infectivity in the culture medium was determined by focus formation assay at 48, 72, and 96 h after transfection. Only positively detected data are shown in the figure. All assays in this figure were performed in duplicate, and the average data are represented.

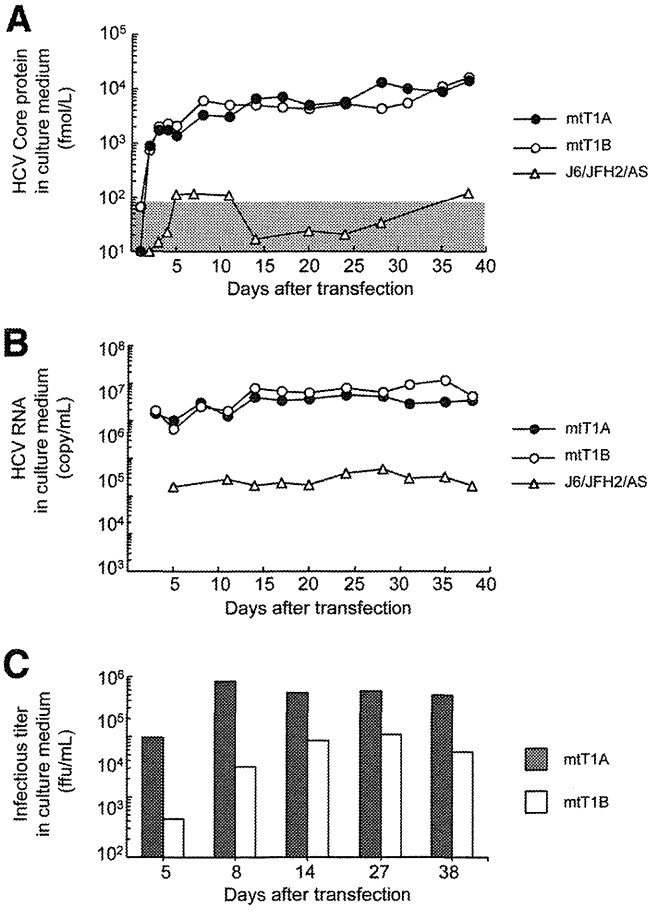

FIG 10 Continuous passage of J6/JFH2/AS cell culture-adapted virus RNA-transfected cells. Full-length HCV RNA was synthesized from the J6/JFH2/AS, J6/JFH2/AS/mtT1A (mtT1A), and J6/JFH2/AS/mtT1B (mtT1B) constructs. RNA-transfected cells were serially passaged until 38 days after transfection, and culture supernatants were harvested at the indicated time points. HCV core protein (A) and HCV RNA (B) levels in the culture media were determined. The data in the gray area were below the detection limit of the assay to detect HCV core protein. (C) Infectivity in the culture medium was determined by focus formation assay at 5, 8, 14, 27, and 38 days after transfection.

also used for electron microscopy analysis. After the density gradient purification, spherical viral particles were detected (Fig. 7, right panel). After the core protein levels plateaued, naive Huh-7.5.1 cells were inoculated with the culture medium, as described above. When the core protein levels plateaued again after the third inoculation of T3 and T4 cells, we sequenced the viral genome in the culture medium (T3i3 and T4i3, respectively) to determine the adaptive mutation. We found the following nonsynonymous mutations: 414IT in E2, 1510EG and 1617RQ in NS3, 2006KQ, 2233AV and 2234NS in NS5A, and 2695TI in NS5B of T3i3; and 387VG in E1, 828VA in NS2, 1225RQ and 1283RG in NS3, 1883VA in NS4B, 2206SA, 2279KN, and 2441CR in NS5A, and 2695TI in NS5B of T4i3 (Fig. 3B). We introduced these mutations into the pJFH2/AS plasmid (pJFH2/AS/mtT3 and pJFH2/AS/mtT4). Synthesized RNA from pJFH2/AS/mtT3 and pJFH2/AS/mtT4 and the related control plasmids was transfected into Huh-7.5.1 cells. HCV core protein levels, HCV RNA levels, and infectivity were monitored in the culture medium of the transfected cells until 96 h after transfection (Fig. 9A to C). JFH2/AS/mtT3 (mtT3) and JFH2/AS/mtT4 (mtT4) secreted similar levels of HCV core protein, RNA, and infectious virus with J6/JFH2/AS/mtT1A and J6/JFH2/AS/mtT1B. Although JFH2/AS/mtT3 secreted slightly higher levels of HCV core protein and RNA than JFH2/AS/mtT4, the secreted infectious virus titers were similar for both viruses. JFH2/AS/mtT3 and JFH2/AS/mtT4 RNA-transfected cells were also serially passaged, and the HCV core proteins were secreted immediately after transfection (Fig. 14A). However, JFH2 and JFH2/AS RNA-transfected cells did not secrete significant amounts of HCV core protein into the culture medium. HCV RNA levels in the culture medium of the RNA-transfected cells were at similar levels for JFH2/AS/mtT3 and JFH2/AS/mtT4 (around 10^7 copy/ml) (Fig. 14B). Infectivity was also detected as higher than 10^4 FFU/ml even at 3 days after the RNA transfection, and this level of infectious titer was maintained during the cell passages (Fig. 14C). We also analyzed JFH2/AS/mtT3 and JFH2/AS/mtT4 culture media by density gradient assay (Fig. 14D). The density profiles with HCV core protein and RNA levels and infectious titers in the fractions were basically similar to those of J6/JFH2/AS-adapted viruses (Fig. 6E and 11D). Taken together, the results described in this section indicate infectious virus was also recovered from the full-length JFH-2 construct with the 2217AS mutation.

Mechanistic analysis of adaptive mutations introduced in the J6/JFH2/AS and JFH2/AS cell culture-adapted viruses. To elucidate the mechanisms of adaptive mutations discovered in J6/JFH2/AS and JFH2/AS virus genomes, we transfected JFH-2 and J6/JFH2 constructs along with possible control constructs into Huh7-25 cells (2) (Fig. 15), which are CD81 defective. The transfection of JFH-1 RNA into Huh7-25 cells results in infectious HCV production, but there was no reinfection into Huh7-25 cells because the cell surface expression of CD81 is essential for HCV infection (10). HCV core protein levels were measured in the culture medium and cell lysate to monitor virus particle secretion and intracellular virus genome replication, respectively (Fig. 15A and B). JFH2/AS, JFH2, J6/JFH2, JFH1/GND, and J6/JFH2/GND RNA-transfected cells did not show increased levels of intracellular core protein expression. However, other RNA-transfected cells showed increased intracellular core protein expression. The cellular core protein level was especially increased at 72 and 96 h after transfection with J6/JFH2/AS RNA, which suggests a higher replication efficiency than J6/JFH; however, core protein secretion was not detected with J6/JFH2/AS, which suggests defective virus particle formation or secretion. Other adaptive mutations in J6/JFH2/AS/mtT1A and J6/JFH2/AS/mtT1B further increased virus genome replication and core protein secretion. In the case of JFH2/AS RNA transfection, cellular core protein expression was not detected, suggesting a lower replication efficiency than that of J6/JFH2/AS. This lower replication efficiency of JFH2/AS may be due to the presence of different sequences in the region of core protein to NS2. However, core protein expression in the cell lysate and culture medium was detected with both JFH2/AS/mtT3 and JFH2/AS/mtT4 RNA transfection. Thus, adaptive mutations in mtT3 and mtT4 are necessary to increase viral genome replication and efficient core protein secretion. JFH-1 and J6/JFH-1 had intracellular core protein expression levels that were similar and high. From the intracellular core protein data, it is clear that J6/JFH2/AS/mtT1A, J6/JFH2/AS/mtT1B, JFH2/AS/mtT3, and JFH2/AS/mtT4 constructs obtained higher replication capacities by

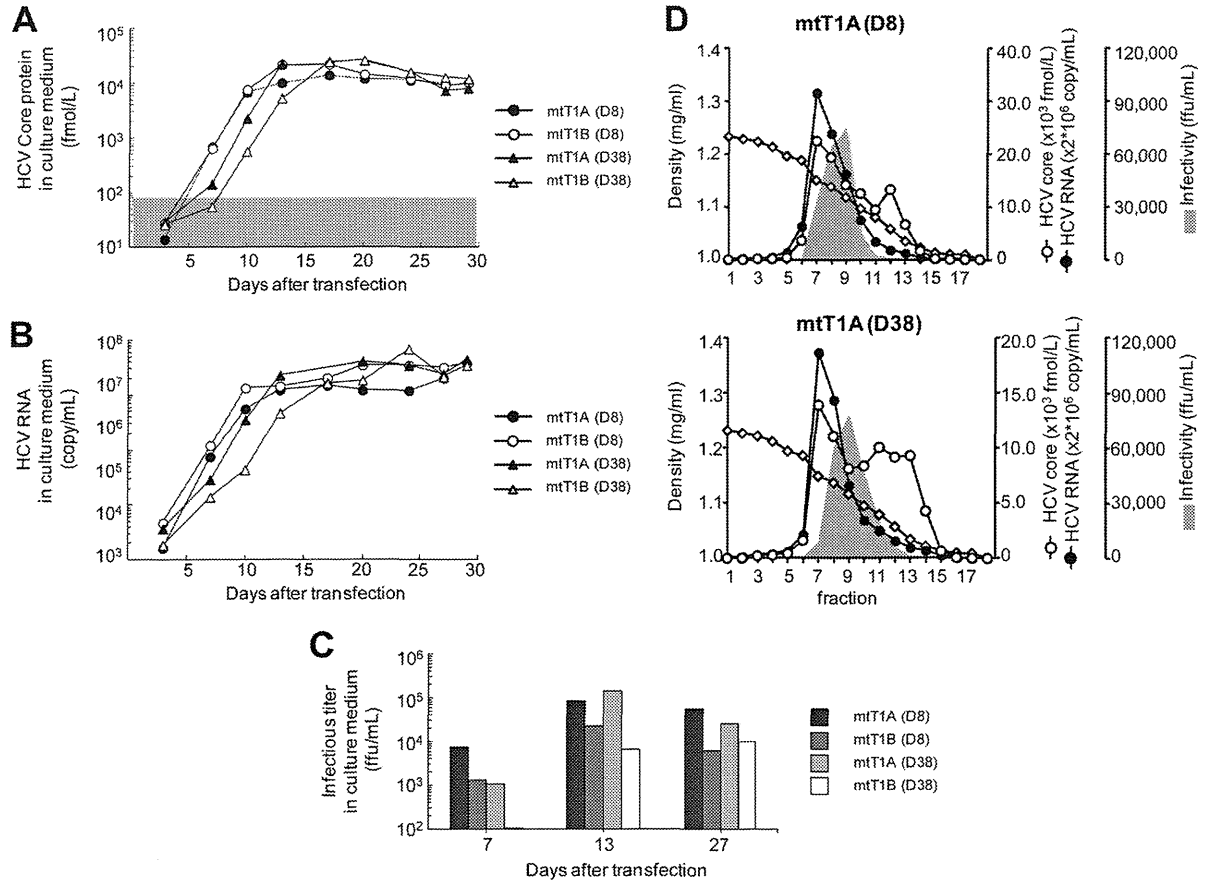

FIG 11 Serial passages of J6/JFH2/AS cell culture-adapted virus infected cells. Naive Huh-7.5.1 cells were inoculated with culture medium of the RNA-transfected cells at an MOI of 0.01. Inoculated cells were serially passaged, and culture supernatants were harvested at the indicated times. HCV core protein (A), HCV RNA (B), and infectivity (C) levels in the culture media were determined. (D) Density gradient analysis of culture supernatant from J6/JFH2/AS/mtT1A cell-culture adapted virus-infected Huh-7.5.1 cells. Culture supernatant of infected Huh-7.5.1 cells with mtT1A (day 8 [D8] D38 posttransfection) was harvested at 20 days after inoculation. Assays were performed as described in the legend of Fig. 6E. Open diamond, buoyant density.

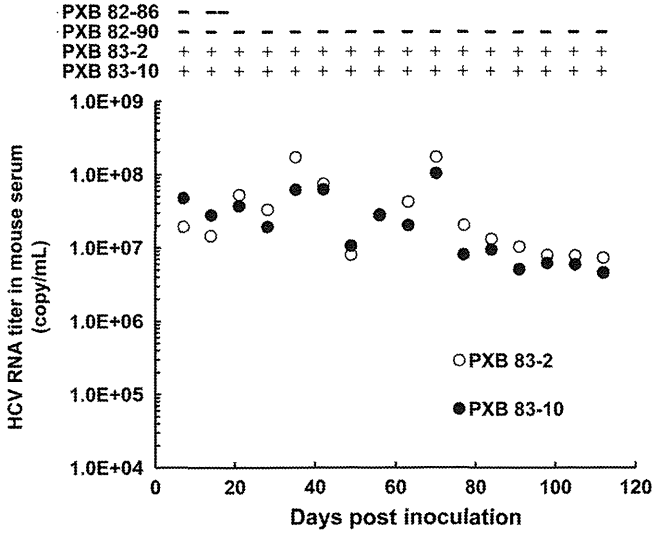

FIG 12 Serum HCV RNA titer in human hepatocyte-transplanted uPA/SCID mice inoculated with JFH-2 serum and cell culture-adapted virus. Mice PXB 82-86 and PXB 82-90 were inoculated with the cell culture-adapted J6/JFH2/AS HCV particles, and mice PXB 83-2 and PXB 83-10 were inoculated with JFH-2 patient serum. Upper and lower panels indicate the results of the RT-PCR and the quantitative detection RT-PCR of HCV RNA in mouse serum, respectively.

adaptive mutations; however, their replication levels are lower than those of JFH-1 and J6/JFH1.

We also analyzed the ratio of extracellular protein to total core protein to analyze the virus secretion efficiency (Fig. 15C). J6/JFH-1 secreted a higher percentage of core protein into culture

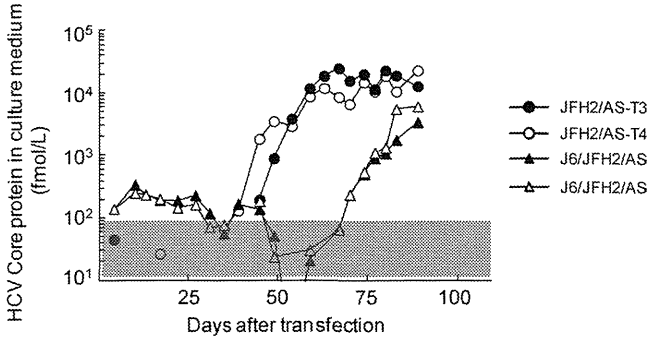

FIG 13 Propagation of a full-length JFH2 virus. Huh-7.5.1 cells were transfected with the transcribed RNA from pJFH2/AS and pJ6/JFH2/AS. Two independently JFH2/AS RNA-transfected cell lines (T3 and T4) were independently passaged. At each time point, culture medium was harvested and analyzed for the presence of HCV core protein.

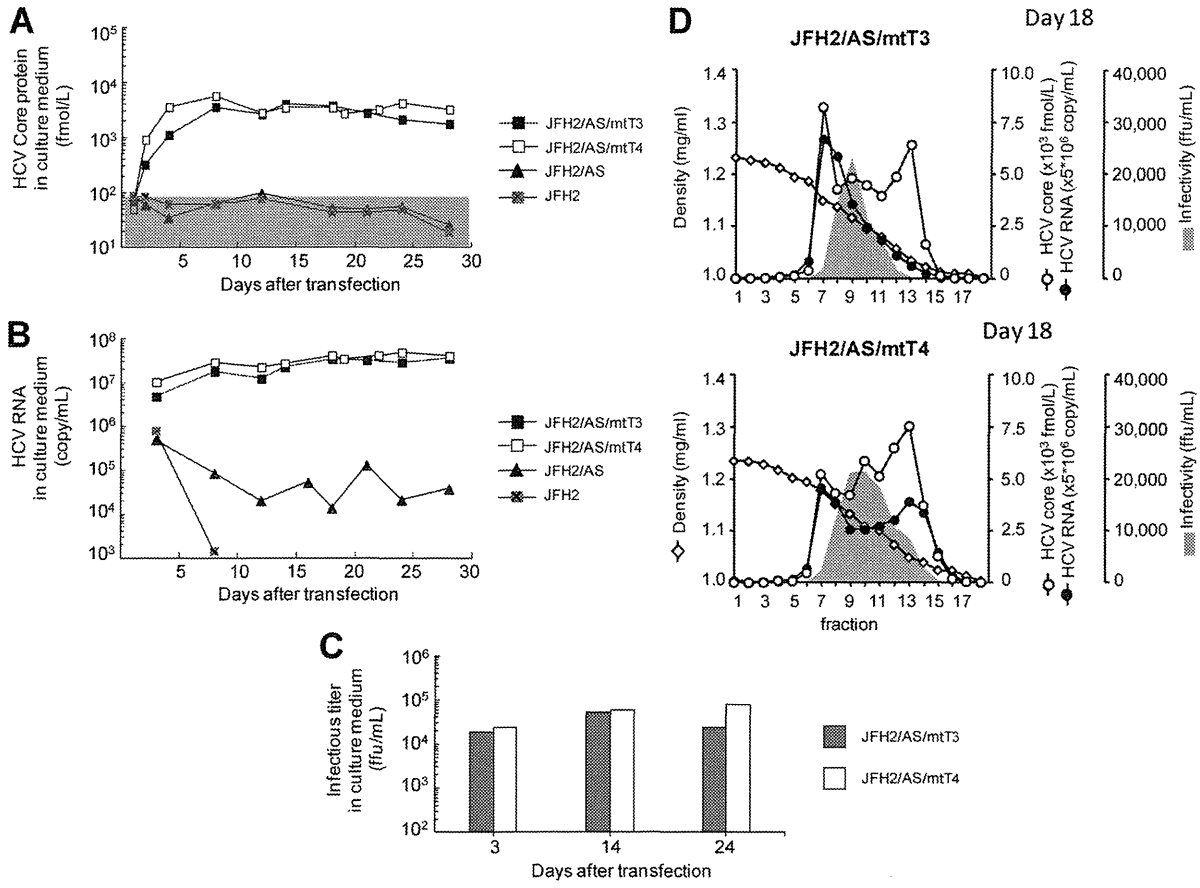

FIG 14 Full-length RNA was synthesized from the JFH2 construct and its derivatives with mutations. RNA-transfected cells were serially passaged, and culture supernatants were harvested at the indicated time points. HCV core protein (A), HCV RNA (B), and infectivity (C) levels in the culture media were determined. The data in the gray area were below the detection limit of the assay to detect HCV core protein. (D) Density gradient analysis of culture supernatant from JFH2/AS cell-culture adapted virus-infected Huh-7.5.1 cells. Culture supernatants of Huh-7.5.1 cells infected with JFH2/mtT3 and JFH2/mtT4 viruses were harvested 18 days after inoculation. Assays were performed as described in the legend of Fig. 6E. Open diamond, buoyant density.

medium than JFH-1. J6/JFH2/AS/mtT1A, J6/JFH2/AS/mtT1B, JFH2/AS/mtT3, and JFH2/AS/mtT4 RNA-transfected cells showed different percentages of secreted core protein. mtT1A and mtT1B constructs showed similar replication levels (Fig. 15B), but mtT1B showed a higher percentage of core protein secretion than mtT1A (Fig. 15C). mtT3 and mtT4 showed similar percentages of core protein secretion, which are higher than the level of JFH1 (Fig. 15C). Because J6/JFH2/AS RNA-transfected cells did not secrete core protein despite intracellular core protein expression (Fig. 15A and B), the adaptive mutant constructs obtained core protein (or virus particle) secretion phenotypes. Thus, during the adaptation process, the viruses obtained both higher replication capacity and core protein secretion capacity by their adaptive mutations.

Other HCV constructs with the 2217AS mutation. The alanine residue at amino acid position 2217 is located in the ISDR of NS5A, and it is conserved among HCV strains including genotype 1 and 2 strains. Because the 2217AS mutation in NS5A is the key mutation for the production of cell culture-adapted HCV, we introduced this mutation into other wild-type HCV constructs, i.e., H77 (genotype 1a), Con1 (genotype 1b), and J6CF (genotype 2a). Synthetic RNAs including the 2217AS mutation were electroporated into Huh-7.5.1 cells, and then the transfected cells were serially passaged. HCV core protein secretion was measured in the culture medium of transfected cells. However, we could not observe the increment of HCV core levels in the culture medium (data not shown). Therefore, we concluded that the 2217AS mutation does not always induce cell culture adaptation in HCV isolates.

DISCUSSION

In previous studies, we have isolated cell culture-infectious HCV, the JFH-1 strain, from a patient with fulminant hepatitis (14, 38). In this report, we isolated another HCV cDNA, named JFH-2, also from a fulminant hepatitis patient. We constructed a subgenomic replicon with the JFH-2 sequence, but its replication efficiency was low. Among the mutations found in the replicon genome, the 2217AS mutation in the ISDR exhibited the strongest adaptive effect. Interestingly, the full-length chimeric or wild-type JFH-2 genome with adaptive mutations could replicate and produce infectious virus particles. Virus infection efficiency was sufficient for autonomous virus propagation in cultured cells.

Several full-length HCV cDNAs have been cloned, and their infectivity has been confirmed *in vivo* with chimpanzee models (18, 39). However, it has been difficult to produce recombinant viral particles and test their infectivity by using cell culture

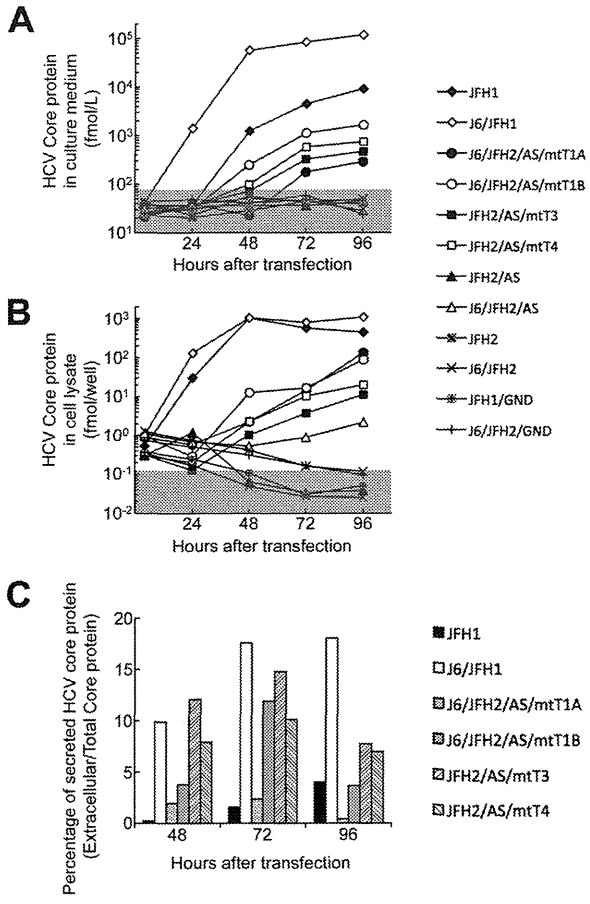

FIG 15 Transient virus production assay of J6/JFH2- and JFH2-related constructs with CD81-defective Huh7-25 cells. Full-length HCV RNA was synthesized from the JFH1, J6/JFH1, JFH2, and J6/JFH2 constructs and their derivatives with mutations and transfected into Huh7-25 cells. (A) HCV core protein levels in culture medium were determined at 4, 24, 48, 72, and 96 h after transfection. The data in the gray area were below detection limit. (B) HCV core protein levels in the cell lysate were determined at 24, 48, 72, and 96 h after transfection. (C) Percentages of secreted HCV core protein from the transfected cells were determined at 48, 72, and 96 h after transfection. Percentages of secreted HCV core protein were calculated only for the indicated viruses. All assays were performed in duplicate, and the data represent average values.

systems (4, 28). Only the JFH-1 strain efficiently replicates in HuH-7 cells and other hepatic and nonhepatic cell lines in subgenomic replicon form (20, 38, 41). Full-length wild-type JFH-1 RNA and chimeric JFH-1 RNA can replicate in HuH-7 cells and produce infectious virus. Since the JFH-1 strain was isolated from a patient with fulminant hepatitis, we assumed that virus strains that cause fulminant hepatitis may replicate efficiently in cultured cells. To identify more HCV clones that can replicate in cultured cells, we isolated the JFH-2 strain from another fulminant hepatitis patient (15). Interestingly, the JFH-2 strain showed a low level of replication in cultured cells in the initial subgenomic replicon experiment. This result may suggest that HCV strains isolated from fulminant hepatitis patients are able to replicate more efficiently than strains from chronic hepatitis patients; however, this hypothesis should be confirmed by testing more HCV strains from patients with fulminant hepatitis. The JFH-2 patient received a course of betamethasone therapy and developed fulminant hepatitis after the withdrawal of betamethasone. It is thus possible that the JFH-2 strain obtained its higher replication capacity in the immune-suppressed host environment. To confirm this hypothesis, we must test the replication efficiency of HCV strains isolated from other immune-suppressed patients, such as patients who are coinfected with HIV, patients who are reinfected after a transplant, and patients who are treated with immunosuppressive agents.

In previous reports, adaptive mutations have been found to enhance viral RNA replication at the expense of virus particle formation efficiency (28). A highly cell culture-adapted Con1 strain can replicate in cultured cells, but it cannot produce infectious virus particles. Interestingly, a highly adapted Con1 strain was not infectious for chimpanzees, while moderately adapted Con1 was infectious. However, the virus recovered from the infected animal was wild-type Con1 virus (5). This result clearly suggests that HCV strains with lower replication efficiencies are favorable for *in vivo* infection. However, we must note that the "replication efficiency" is determined in cultured cells. In the case of JFH-2, we found several adaptive mutations in the subgenomic replicon clones, and the most adaptive mutation, 2217AS, was tested in full-length HCV replication and virus production. After the RNA transfection of J6/JFH2/AS, we could not detect substantial virus secretion for about 30 days. However, after 30 days, significant levels of infectious virus particles were secreted into the culture medium. Naive Huh-7.5.1 cells were inoculated three times with the cell culture-adapted virus. This virus adaptation was also tested with full-length JFH2/AS, and we successfully obtained infectious JFH2/AS virus. Both the J6/JFH2/AS and JFH2/AS viruses acquired the ability for autonomous virus expansion in Huh-7.5.1 cells, and several additional mutations were found in their genomes. Interestingly, the 2695TI mutation in NS5B was commonly found in all of the adapted virus genomes, and isoleucine at amino acid position 2695 is also found in the JFH-1 strain. However, the introduction of only the 2695TI mutation into the J6/JFH2/AS or JFH2/AS virus genome did not restore robust virus production (data not shown). After repeated virus passages, mutations were found throughout the viral genome (in J6/JFH2/AS-T1Ai3 and -T1Bi3 and in JFH2/AS-T3i3 and -T4i3), and we are currently investigating which mutations or combinations of mutations are most important for this adaptation. From the comparisons of cell culture-adapted viruses and their parental virus constructs, adaptive mutations are necessary to increase both viral genome replication and virus particle assembly/secretion efficiency (Fig. 15). The procedure to produce cell culture-adapted HCV was thus established. The adaptive mutations found from the subgenomic replicon assay were introduced into the full-length genome, and the cells transfected with virus RNA were repeatedly passaged until the virus particles were produced.

In vivo infectivity may be inversely related to the replication efficiency in cultured cells, as discussed above. The original JFH-2 patient serum was infectious in human liver-transplanted mice; however, cell culture-adapted J6/JFH2/AS virus was not infectious. The JFH-1 virus was infectious not only for cultured cells but also for chimpanzees and human liver-transplanted mice (10, 38). However, the JFH-1 infection in chimpanzees was only mild and transient without any liver pathology. Thus, the J6/JFH2/AS and JFH2/AS viruses are more cell culture-adapted and attenuated than the JFH-1 virus. It may be worthwhile to test this cell culture-

adapted strain as a live attenuated vaccine candidate to induce protective immunity. However, for ethical reasons, the necessary chimpanzee experiments are not appropriate to perform. Therefore, we should wait for the establishment of immunocompetent small-animal models susceptible to HCV infection to perform this kind of study. Furthermore, future studies should examine the *in vivo* infectivity of the adapted J6/JFH2 and JFH2 viruses isolated in the present study.

The 2217AS mutation is located in the ISDR. In the previous study of the genotype 1b subgenomic replicon, mutations introduced into the ISDR enhanced the colony formation efficiency of the HCV replicons (17, 23). However, mutations in the ISDR impaired the genotype 1b HCV replication in human liver-transplanted mice (9). The exact mechanism of the ISDR is still not clear although the number of mutations in the ISDR is related to the efficacy of interferon therapy (8). Our results in this study also support the concept that the 2217AS mutation in the ISDR enhances replicon replication efficiency although the J6/JFH2/AS virus did not infect human liver-transplanted mice. Further studies are necessary to understand the molecular mechanism of the effects of adaptive mutations in the ISDR.

In the present study, we established a cell culture-adapted HCV strain, JFH-2. The virus could be passaged continuously in naive Huh-7.5.1 cells. This approach may be applicable to the establishment of new infectious HCV clones. Novel antiviral drugs are under development, and some of them will be used in the clinical setting. However, most of them target genotype 1 HCV strains. To eradicate other genotypes of HCV, it is important to establish their replicons and infectious virus culture systems.

ACKNOWLEDGMENTS

Huh-7.5.1 cells were kindly provided by Francis V. Chisari. The J6CF plasmid was a kind gift from Jens Bukh. Anti-HCV human IgG was a kind gift from Hiroshi Yoshizawa and Junko Tanaka, Hiroshima University. AP33 antibody was generously provided by Genentec. We thank Tetsuro Suzuki and Hideki Aizaki for their helpful discussions. We also thank Minako Kaga for her technical assistance.

This work was partially supported by Grants-in-Aid for Scientific Research from the Japan Society for the Promotion of Science, from the Ministry of Health, Labor and Welfare of Japan, from the Ministry of Education, Culture, Sports, Science and Technology, from the National Institute of Biomedical Innovation, and by the Research on Health Sciences Focusing on Drug Innovation from the Japan Health Sciences Foundation.

REFERENCES

1. **Aizaki H, et al.** 2008. Critical role of virion-associated cholesterol and sphingolipid in hepatitis C virus infection. J. Virol. **82**:5715–5724.
2. **Akazawa D, et al.** 2007. CD81 expression is important for the permissiveness of Huh7 cell clones for heterogeneous hepatitis C virus infection. J. Virol. **81**:5036–5045.
3. **Akazawa D, et al.** 2011. Production and characterization of HCV particles from serum-free culture. Vaccine **29**:4821–4828.
4. **Bartenschlager R, Lohmann V.** 2000. Replication of hepatitis C virus. J. Gen. Virol. **81**:1631–1648.
5. **Bukh J, et al.** 2002. Mutations that permit efficient replication of hepatitis C virus RNA in Huh-7 cells prevent productive replication in chimpanzees. Proc. Natl. Acad. Sci. U. S. A. **99**:14416–14421.
6. **Choo QL, et al.** 1989. Isolation of a cDNA clone derived from a blood-borne non-A non-B viral hepatitis genome. Science **244**:359–362.
7. **Di Bisceglie AM, Hoofnagle JH.** 2002. Optimal therapy of hepatitis C. Hepatology **36**:S121–S127.
8. **Enomoto N, et al.** 1995. Sensitivity to interferon is conferred by amino acid substitutions in the NS5A region. J. Clin. Invest. **96**:224–230.
9. **Hiraga N, et al.** 2011. Impact of viral amino acid substitutions and host interleukin-28b polymorphism on replication and susceptibility to interferon of hepatitis C virus. Hepatology **54**:764–771.
10. **Kato T, et al.** 2008. Hepatitis C virus JFH-1 strain infection in chimpanzees is associated with low pathogenicity and emergence of an adaptive mutation. Hepatology **48**:732–740.
11. **Kato T, et al.** 2003. Efficient replication of the genotype 2a hepatitis C virus subgenomic replicon. Gastroenterology **125**:1808–1817.
12. **Kato T, et al.** 2005. Detection of anti-hepatitis C virus effects of interferon and ribavirin by a sensitive replicon system. J. Clin. Microbiol. **43**:5679–5684.
13. **Kato T, et al.** 2006. Cell culture and infection system for hepatitis C virus. Nat. Protoc. **1**:2334–2339.
14. **Kato T, et al.** 2001. Sequence analysis of hepatitis C virus isolated from a fulminant hepatitis patient. J. Med. Virol. **64**:334–339.
15. **Kato T, et al.** 2003. Processing of hepatitis C virus core protein is regulated by its C-terminal sequence. J. Med. Virol. **69**:357–366.
16. **Kiyosawa K, et al.** 1990. Interrelationship of blood transfusion, non-A, non-B hepatitis and hepatocellular carcinoma: analysis by detection of antibody to hepatitis C virus. Hepatology **12**:671–675.
17. **Kohashi T, et al.** 2006. Site-specific mutation of the interferon sensitivity-determining region (ISDR) modulates hepatitis C virus replication. J. Viral Hepat. **13**:582–590.
18. **Kolykhalov AA, et al.** 1997. Transmission of hepatitis C by intrahepatic inoculation with transcribed RNA. Science **277**:570–574.
19. **Kuo G, et al.** 1989. An assay for circulating antibodies to a major etiologic virus of human non-A non-B hepatitis. Science **244**:362–364.
20. **Lindenbach BD, et al.** 2005. Complete replication of hepatitis C virus in cell culture. Science **309**:623–626.
21. **Lindenbach BD, et al.** 2006. Cell culture-grown hepatitis C virus is infectious in vivo and can be recultured in vitro. Proc. Natl. Acad. Sci. U. S. A. **103**:3805–3809.
22. **Lohmann V, et al.** 1999. Replication of subgenomic hepatitis C virus RNAs in a hepatoma cell line. Science **285**:110–113.
23. **Maekawa S, et al.** 2004. Introduction of NS5A mutations enables subgenomic HCV replicon derived from chimpanzee-infectious HC-J4 isolate to replicate efficiently in Huh-7 cells. J. Viral Hepat. **11**:394–403.
24. **McHutchison JG, et al.** 1998. Interferon alfa-2b alone or in combination with ribavirin as initial treatment for chronic hepatitis C. N. Engl. J. Med. **339**:1485–1492.
25. **Merck & Co.** 2011. Victrelis (boceprevir) prescribing information. Merck & Co., Whitehouse Station, NJ. http://www.accessdata.fda.gov/drugsatfda_docs/label/2011/202258lbl.pdf.
26. **Murayama A, et al.** 2007. The NS3 helicase and NS5B-to-3′X regions are important for efficient hepatitis C virus strain JFH-1 replication in Huh7 cells. J. Virol. **81**:8030–8040.
27. **Murayama A, et al.** 2010. RNA polymerase activity and specific RNA structure are required for efficient HCV replication in cultured cells. PLoS Pathog. **6**:e1000885. doi:10.1371/journal.ppat.1000885.
28. **Pietschmann T, et al.** 2002. Persistent and transient replication of full-length hepatitis C virus genomes in cell culture. J. Virol. **76**:4008–4021.
29. **Pietschmann T, et al.** 2009. Production of infectious genotype 1b virus particles in cell culture and impairment by replication enhancing mutations. PLoS Pathog. **5**:e1000475. doi:10.1371/journal.ppat.1000475.
30. **Poynard T, et al.** 1998. Randomised trial of interferon α2b plus ribavirin for 48 weeks or for 24 weeks versus interferon α2b plus placebo for 48 weeks for treatment of chronic infection with hepatitis C virus. Lancet **352**:1426–1432.
31. **Saeed M, et al.** 2009. Evaluation of hepatitis C virus core antigen assays in detecting recombinant viral antigens of various genotypes. J. Clin. Microbiol. **47**:4141–4143.
32. **Takahashi H, et al.** 2010. Biological properties of purified recombinant HCV particles with an epitope-tagged envelope. Biochem. Biophys. Res. Commun. **395**:565–571.
33. **Tateno C, et al.** 2004. Near completely humanized liver in mice shows human-type metabolic responses to drugs. Am. J. Pathol. **165**:901–912.
34. **U. S. Food and Drug Administration.** 2011. FDA news release. FDA approves Incivek for hepatitis C. U.S. Food and Drug Administration, Silver Spring, MD. http://www.fda.gov/NewsEvents/Newsroom/PressAnnouncements/ucm256299.htm.
35. **U. S. Food and Drug Administration.** 2011. FDA news release. FDA approves Victrelis for hepatitis C. U.S. Food and Drug Administration,

Silver Spring, MD. http://www.fda.gov/NewsEvents/Newsroom/PressAnnouncements/ucm255390.htm.
36. **Vertex Pharmaceuticals.** 2011. Incivek (telaprevir) prescribing information. Vertex Pharmaceuticals, Cambridge, MA. http://www.accessdata.fda.gov/drugsatfda_docs/label/2011/201917lbl.pdf.
37. **Wakita T.** 2009. Isolation of JFH-1 strain and development of an HCV infection system. Methods Mol. Biol. **510**:305–327.
38. **Wakita T, et al.** 2005. Production of infectious hepatitis C virus in tissue culture from a cloned viral genome. Nat. Med. **11**:791–796.
39. **Yanagi M, Purcell RH, Emerson SU, Bukh J.** 1997. Transcripts from a single full-length cDNA clone of hepatitis C virus are infectious when directly transfected into the liver of a chimpanzee. Proc. Natl. Acad. Sci. U. S. A. **94**:8738–8743.
40. **Yanagi M, Purcell RH, Emerson SU, Bukh J.** 1999. Hepatitis C virus: an infectious molecular clone of a second major genotype (2a) and lack of viability of intertypic 1a and 2a chimeras. Virology **262**:250–263.
41. **Zhong JP, et al.** 2005. Robust hepatitis C virus infection in vitro. Proc. Natl. Acad. Sci. U. S. A. **102**:9294–9299.